Geochemistry Geophysics Geosystems G3

Article
Volume 11, Number 8
4 August 2010
Q08005, doi:10.1029/2010GC003105
ISSN: 1525-2027

Published by AGU and the Geochemical Society

Postspreading rifting in the Adare Basin, Antarctica: Regional tectonic consequences

R. Granot
Scripps Institution of Oceanography, University of California, San Diego, 9500 Gilman Drive, La Jolla, California 92093, USA

Now at Institut de Physique du Globe de Paris, 4 Place Jussieu, F-75005 Paris, France (granot@ipgp.fr)

S. C. Cande
Scripps Institution of Oceanography, University of California, San Diego, 9500 Gilman Drive, La Jolla, California 92093, USA

J. M. Stock
Seismological Laboratory, California Institute of Technology, 1200 East California Boulevard, 252-21, Pasadena, California 91125, USA

F. J. Davey
Institute of Geological and Nuclear Sciences, PO Box 30368, Lower Hutt, New Zealand

R. W. Clayton
Seismological Laboratory, California Institute of Technology, 1200 East California Boulevard, 252-21, Pasadena, California 91125, USA

[1] Extension during the middle Cenozoic (43–26 Ma) in the north end of the West Antarctic rift system (WARS) is well constrained by seafloor magnetic anomalies formed at the extinct Adare spreading axis. Kinematic solutions for this time interval suggest a southward decrease in relative motion between East and West Antarctica. Here we present multichannel seismic reflection and seafloor mapping data acquired within and near the Adare Basin on a recent geophysical cruise. We have traced the ANTOSTRAT seismic stratigraphic framework from the northwest Ross Sea into the Adare Basin, verified and tied to DSDP drill sites 273 and 274. Our results reveal three distinct periods of tectonic activity. An early localized deformational event took place close to the cessation of seafloor spreading in the Adare Basin (~24 Ma). It reactivated a few normal faults and initiated the formation of the Adare Trough. A prominent pulse of rifting in the early Miocene (~17 Ma) resulted in normal faulting that initiated tilted blocks. The overall trend of structures was NE–SW, linking the event with the activity outside the basin. It resulted in major uplift of the Adare Trough and marks the last extensional phase of the Adare Basin. Recent volcanic vents (Pliocene to present day) tend to align with the early Miocene structures and the on-land Hallett volcanic province. This latest phase of tectonic activity also involves near-vertical normal faulting (still active in places) with negligible horizontal consequences. The early Miocene extensional event found within the Adare Basin does not require a change in the relative motion between East and West Antarctica. However, the lack of subsequent rifting within the Adare Basin coupled with the formation of the Terror Rift and an on-land and subice extension within the WARS require a pronounced change in the kinematics of the rift. These observations indicate that extension increased southward, therefore suggesting that a major change in relative plate motion took place in the middle Miocene. The late Miocene pole of rotation might have been located north of the Adare Basin, with opposite opening sign compared to the Eocene-Oligocene pole.

Components: 17,300 words, 16 figures.

Keywords: West Antarctic rift system; rift; Adare Basin; multichannel seismic reflection; magnetic anomalies; tectonics.

Index Terms: 3040 Marine Geology and Geophysics: Plate tectonics (8150, 8155, 8157, 8158); 9310 Geographic Location: Antarctica (4207).

Received 26 February 2010; **Revised** 30 April 2010; **Accepted** 6 May 2010; **Published** 4 August 2010.

Granot, R., S. C. Cande, J. M. Stock, F. J. Davey, and R. W. Clayton (2010), Postspreading rifting in the Adare Basin, Antarctica: Regional tectonic consequences, *Geochem. Geophys. Geosyst.*, *11*, Q08005, doi:10.1029/2010GC003105.

1. Introduction

[2] The West Antarctic rift system (WARS) separates cratonic East Antarctica from younger blocks that assembled to form West Antarctica in the late Mesozoic [*Elliot*, 1992; *Heimann et al.*, 1994] (Figure 1). Cenozoic rifting has probably influenced the denudation history of the Transantarctic Mountains, the uplifted rift flank of the WARS [e.g., *Fitzgerald and Stump*, 1997; *ten Brink et al.*, 1997], and consequently influenced the growth of the Antarctic cryosphere [*Behrendt and Cooper*, 1991; *Van der Wateren and Cloetingh*, 1999]. The WARS also plays an important role in the global plate circuit and has long been recognized as a missing link in many plate reconstruction models [e.g., *Molnar et al.*, 1975]. There is still considerable debate regarding the kinematic history of the rift for most of its existence [e.g., *Storti et al.*, 2007; *Karner et al.*, 2005].

[3] The Adare Basin, located north of the western Ross Sea (Figure 1), was formed along a seafloor spreading center [*Cande et al.*, 2000] that was active between chrons C20 and C9 (middle Eocene to late Oligocene, 43 to 26 Ma [*Cande and Kent*, 1995]). Structural continuity between the Adare Basin and Northern Basin [e.g., *Cande and Stock*, 2006] implies that the kinematic solutions calculated for the Adare seafloor spreading [*Cande et al.*, 2000; *Davey et al.*, 2006] provide crucial constraints for the Eocene-Oligocene motions of the entire rift system. The postspreading extensional activity within the Adare Basin, as recorded by sediments, bathymetry, and offset of magnetic lineations, may therefore provide valuable insights on the late Oligocene and Neogene (<26 Ma) kinematics of the WARS, a poorly resolved period in the history of the rift.

[4] Here we present a grid of multichannel seismic (MCS) reflection data as well as bathymetric mapping results from geophysical cruise NBP0701 aboard the R/VIB *Nathaniel B. Palmer*. We first present a correlation of seismic stratigraphic units from the Northern Basin into the Adare Basin following the stratigraphic framework set by *Brancolini et al.* [1995], which we verified and tied to DSDP drill sites 273 and 274. Although our approach suffers from notable limitations, particularly for the oldest, late Oligocene parts of the section, it still yields important temporal constraints on the Neogene evolution of the Adare Basin. We then assess the tectonic evolution of the Adare Basin and identify three major tectonic events: (1) a localized fault reactivation event that occurred near the end of seafloor spreading (~24 Ma), (2) an early Miocene (~17 Ma) localized extensional event characterized by tilted blocks and normal faulting, and (3) a period of Pliocene to present-day (<5 Ma) extensive volcanism that, together with near-vertical normal faults, marks the last phase of deformation in the Adare Basin. We then discuss the implications of our results for the kinematics of the WARS during the Neogene. Finally, we conclude with a comparison of our results to the regional kinematic framework.

2. Tectonic Setting and History of the West Antarctic Rift System

[5] The initial stages of rifting between East and West Antarctica are characterized by spatially and temporally diffuse deformation. The middle Jurassic continental flood basalts of the Ferrar Group, found along the Transantarctic Mountains, provide the oldest evidence for the breakup of Gondwanaland [*Heimann et al.*, 1994]. Paleomagnetic measurements suggest that there has been a total of 500 to 1000 km of transtensional motion between West and East Antarctica since middle Cretaceous [*Divenere et al.*, 1994; *Luyendyk et al.*, 1996]. Reworked Cretaceous marine sediments [*Truswell and Drewry*, 1984] and dredged mylonites [*Siddoway et al.*, 2004] mark the late Mesozoic

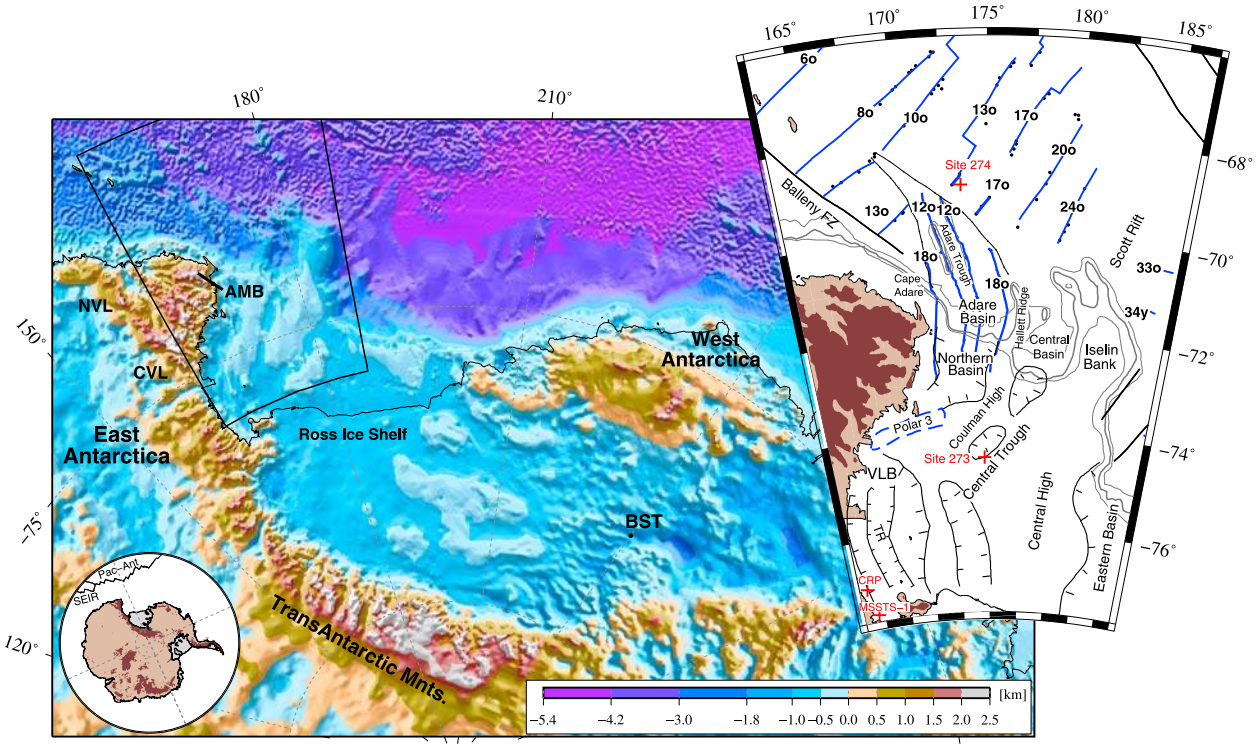

Figure 1. Tectonic setting and location map of the West Antarctic rift system. Elevation and bathymetry are based on the BEDMAP compilation of *Lythe and Vaughan* [2001]. Large inset shows the main structural elements of the Adare Basin and western Ross Sea. Blue lines delineate magnetic lineations. Anomalies 18o and 12o run continuously from the Adare Basin into the Northern Basin (based on archival shipboard magnetic data and aeromagnetic data of *Damaske et al.* [2007]). Dashed blue line denotes a large magnetic anomaly (Polar 3). Locations of drill sites are shown with red crosses. Gray lines delineate the 1000, 1500, and 2000 m contours. NVL, Northern Victoria Land; AMB, Admiralty Mountains Block; CVL, Central Victoria Land; BST, Bentley Subglacial Trench; SEIR, South East Indian Ridge; Pac-Ant, Pacific-Antarctic ridge; VLB, Victoria Land Basin; TR, Terror Rift.

phase of broad subsidence and rifting of the Ross Sea sector that is linked to the progressive fragmentation of Gondwanaland. During the late Cretaceous and early Cenozoic, N–S trending basins (Eastern Basin, Central Trough, Victoria Land Basin, and its northern continuation, Northern Basin) and ridges (Coulman and Central Highs) were formed within the Ross Embayment (Ross Sea and Ross Ice Shelf [*Cooper et al.*, 1987]) (Figure 1). Extension north of the Ross Sea may have been partly accommodated by counterclockwise rotations of the Central Basin and Iselin Bank sector [*Cande and Stock*, 2004a]. During the same time interval (late Mesozoic), termination of subduction underneath Gondwanaland initiated a broad upwelling flow of mantle material that resulted in a region of anomalous shallow bathymetry adjacent to the Ross Sea [*Sutherland et al.*, 2010].

[6] Additional middle Cenozoic opening and subsidence was focused in the western Ross Sea (Northern Basin and Victoria Land Basin [*Cooper and Davey*, 1985; *Davey and Brancolini*, 1995]) (Figure 1). Total extension within the Victoria Land Basin (VLB) was estimated to be 95 km [*Davey and De Santis*, 2006]. Fission track dating of basement apatite suggests that this phase of rifting was accompanied by an increase in denudation rates of the Transantarctic Mountains [*Fitzgerald et al.*, 1986; *Gleadow and Fitzgerald*, 1987].

[7] The transition from the early Cenozoic diffuse extension to the localization of rifting in the western part of the Ross Sea is consistent with a thermal evolution model of the rift zone where progressive cooling and hardening have led to lithospheric necking along the East Antarctic plate boundary [*Huerta and Harry*, 2007]. Alternatively, although not required by numerical models, localization of deformation may have been driven by changes in plate motions [*Wilson*, 1995] or by the impingement of a mantle plume [*Behrendt et al.*, 1994]. Based on extensive on-land and limited offshore seismic observations, inferred major NW–SE dextral

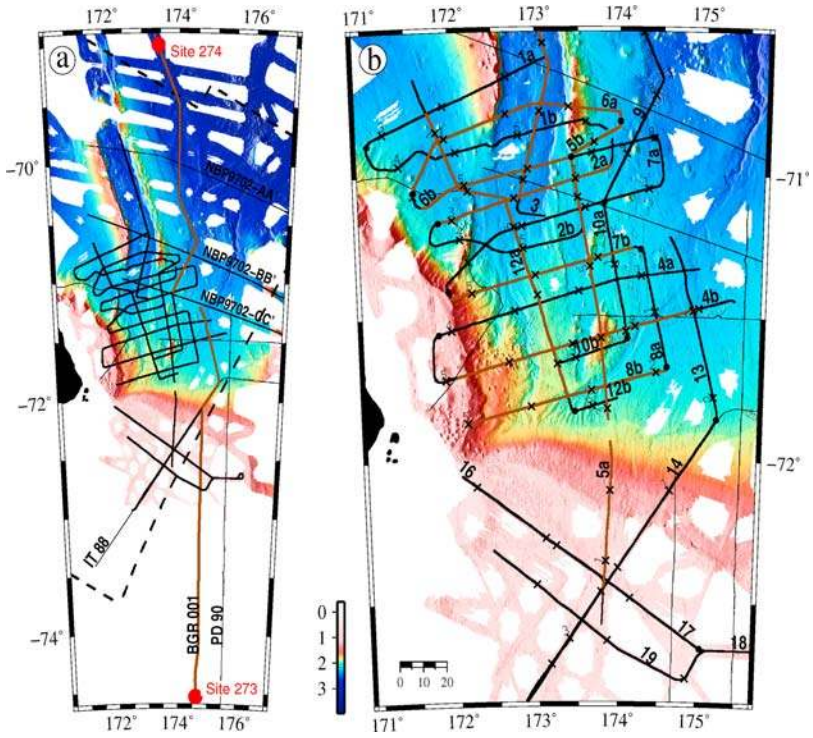

Figure 2. Bathymetric maps of the Adare and Northern basins. Locations of archival seismic reflection profiles are shown with thin black lines. MCS profiles collected during NBP0701 cruise are delineated with thick black lines. Brown lines highlight the sections of the profiles shown within this manuscript. (a) Locations of the tie lines from DSDP drill sites 273 and 274. The boundaries of the aeromagnetic survey conducted as part of GANOVEX IX 2005–2006 [*Damaske et al.*, 2007] are shown with dashed black lines. Note that Line 14 of NBP0701 runs along the archive Line IT 88. (b) Close-up map showing NBP0701 MCS grid lines. Black crosses indicate the location of every thousandth shot point, labeled every 2000 shot points. The profiles presented in this manuscript are ordered as follows: first, we show the tie lines (Figures 4 and 5); then, the profiles are shown with respect to their latitudinal locations, starting from the north (Figure 6, Line 6a) and ending at the south (Figure 11, Line 8b). Two additional N–S profiles are presented in Figures A1 and A2 (Lines 12a and 3).

strike-slip intraplate faults in the northern Victoria Land have been suggested to crosscut the N–S structures [e.g., *Salvini et al.*, 1997; *Rossetti et al.*, 2006; *Storti et al.*, 2007]. These studies have argued that NW–SE dextral strike-slip motion was the dominant mechanism of deformation within and near the Ross Sea sector since Eocene time. Our new data from the Adare Basin, as will be discussed later in the text, do not support this hypothesis.

[8] The best manifestation of the Cenozoic motion between East and West Antarctica lies in the north end of the rift system. There, adjacent to the continental slope from the north, the Adare Basin is located in line with the Northern Basin and is characterized by resolvable linear marine magnetic anomalies (anomalies 11 to 18 [*Cande et al.*, 2000; *Damaske et al.*, 2007]). These anomalies elucidate the fossil Adare spreading center, the slowest arm in a ridge-ridge-ridge triple junction [*Cande et al.*, 2000]. Seafloor spreading took place at nearly constant and asymmetric spreading rates: 7.5 mm/yr and 5 mm/yr in the east and west flanks of the basin, respectively [*Cande et al.*, 2000]. Spreading accounted for 170 km of ENE–WSW plate separation. Continuous magnetic anomalies [*Damaske et al.*, 2007], Bouguer gravity anomalies, and undisrupted sedimentary sequences across the shelf south of the Adare Basin [*Cande and Stock*, 2006] suggest that the opening of the basin was accompanied by the opening of the Northern Basin where massive and focused magmatic intrusions were likely to have been emplaced. Using gravity data and limited seismic reflection data, *Müller et al.* [2005] showed that the formation of the Adare Trough, an uplifted structure located within the Adare Basin (Figure 2, frequently misinterpreted as a remnant of the ridge axis), probably resulted from fault reactivation during the first 5 Myr after spreading stopped. *Müller et al.* [2005] also con-

cluded that no significant extension took place in the Adare Basin afterward, i.e., during the Neogene.

[9] Neogene extensional activity has been accommodated along most of the WARS. The latest phase of extension in the Ross Sea was concentrated in the Terror Rift, a middle Miocene narrow rifted zone located within the center of the VLB [*Cooper et al.*, 1987] (Figure 1). Based on a detailed MCS data set, *Henrys et al.* [2007] estimated that the Terror Rift has accommodated 10 to 15 km of extension since 13 Ma [*Fielding et al.*, 2006, 2008]. A pronounced extensional phase is also evident in the Admiralty Mountains Block, located immediately southwest of the Adare Basin (Figure 1) [*Faccenna et al.*, 2008]. There, a total of 5 km of extension was accommodated along a set of NE–SW to N–S trending normal faults since the middle Miocene [*Faccenna et al.*, 2008]. Further south, *LeMasurier* [2008] has suggested that subice deep troughs and basins filled with thin layers of sediments (Figure 1) [*Anandakrishnan and Winberry*, 2004] were formed underneath the Ross Ice Shelf and West Antarctic ice sheet during the Neogene. These tectonic events were accompanied by an extensive Neogene bimodal volcanic activity similar to that found in the western Ross Sea [*LeMasurier*, 1990].

[10] The currently negligible extensional activity of the rift system significantly differs from the widespread phase of Neogene rifting. Present-day high heat flow [*Blackman et al.*, 1987; *Della Vedova et al.*, 1992] and low seismic velocities in the upper mantle [*Morelli and Danesi*, 2004; *Watson et al.*, 2006] observed within the western Ross Sea have been attributed to the late Cenozoic rifting and thinning of the West Antarctic lithosphere. Yet, lack of seismic activity [*Evison*, 1967; *Behrendt et al.*, 1991] and minor present-day displacements [*Donnellan and Luyendyk*, 2004; *Zanutta et al.*, 2008] testify that the rift system is currently inactive. How the Neogene rifting evolved into the present-day state of inactivity of the WARS still remains to be resolved and is the focus of this work.

3. Data Collection and Processing

[11] We collected a grid of more than 2,700 km of two-dimensional MCS reflection data together with multibeam bathymetric mapping (using Simrad EM 120) within the Adare Basin and across the shelf (Figure 2) in January 2007 during a geophysical cruise aboard the R/VIB *Nathaniel B. Palmer* (NBP0701). The typical line spacing was 20 km. Our new MCS data set is complemented by ~500 km of archival MCS data (available through the Antarctic Seismic Data Library System, http://sdls.ogs.trieste.it/) that allow us to tie the seismic grid to the closest DSDP drill sites 274 and 273 (Figure 2). Additional data collected during the cruise, including sonobuoy refraction, and gravity, will be discussed elsewhere.

[12] Seismic reflection data were acquired with a 1200 m oil-filled streamer. For most of the profiles, the seismic energy source was an array of six generator-injector air guns that were fired in harmonic mode with generator source of 105 cubic inches and injection sources of 105 cubic inches. In the shallower water of the Ross Sea shelf, we used an array of six Bolt air guns with a total capacity of 2125 cubic inches. Data were recorded on 47 (out of 48) channels. The data were 8 s records with 0.002 s sample rate and a shot spacing of approximately 28 m (43 m for the lines collected on the shelf). Processing of the data included velocity semblance analysis every kilometer on common depth point (CDP) gathers. Subsequent processing included stacking and F-K migration. Exponential gain (α = 0.5) was finally applied to increase imaging of the deep structures. For the profiles that crossed the shelf we applied a Time Variant Butterworth Filter and a parabolic Radon transform [*Hampson*, 1986] prior to stacking, to reduce the energy of multiples. These processes resulted in resolvable primary arrivals as deep as ~2.2 s two-way travel time. The final seismic results, together with the archival data, were then imported into Kingdom Suite software for interpretation. Paper prints were also used for interpretation and served as a quality control.

[13] We also made use of aeromagnetic data collected recently as part of GANOVEX IX 2005/06 (see Figure 2a for location of survey [*Damaske et al.*, 2007]). We have identified marine magnetic anomalies (anomalies 12o, 13o, 16y, and 18o) along a total of ~25,000 km of the GPS-navigated magnetic profiles. These picks are used here to delineate the age setting of the Adare crust and to locate and constrain postspreading deformation. A separate study (R. Granot et al., manuscript in preparation, 2010) uses this dense concentration of picks to refine the kinematics of the Adare Basin and WARS during the Eocene-Oligocene interval (43 to 26 Ma).

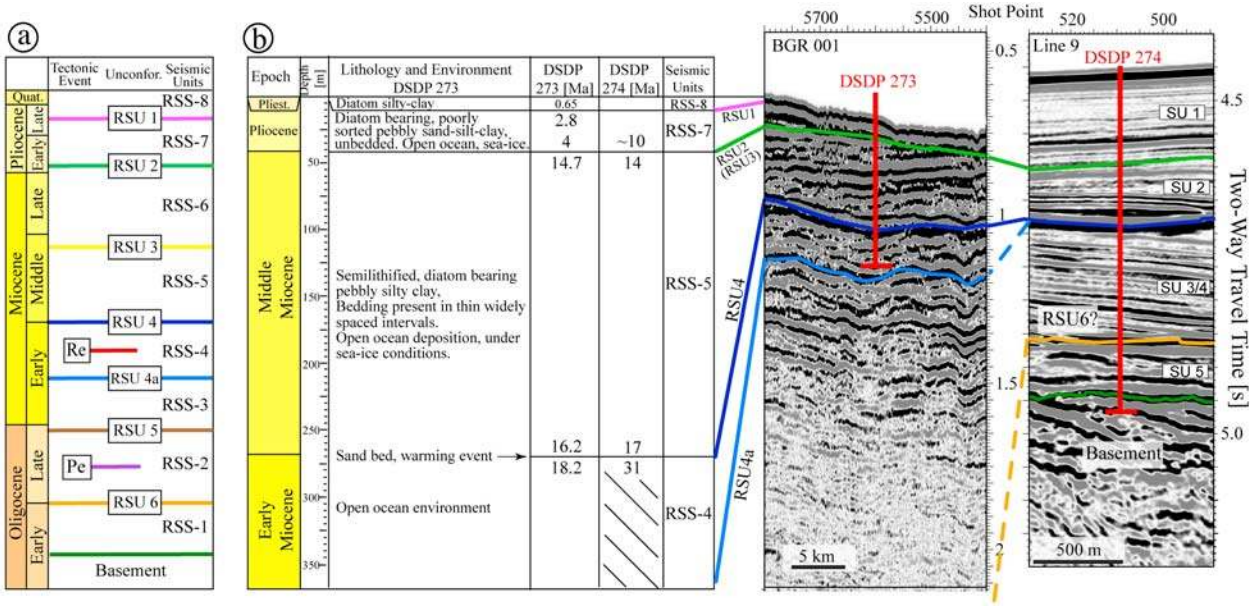

Figure 3. Seismic stratigraphic framework. (a) The stratigraphic framework that was used in this study. This stratigraphic framework was defined by the ANTOSTRAT project [*Brancolini et al.*, 1995] where the Ross Sea seismic sequences (RSS1-8) are divided by the Ross Sea unconformities (RSU6-1). The onsets of the two extensional events described here are marked by Pe ("Purple event," ~24 Ma) and Re ("Red event," ~17 Ma). (b) Correlation of DSDP Site 273 stratigraphic column with DSDP Site 274 and the ANTOSTRAT sequences. The seismic units (SU1-5) that were used in previous stratigraphic studies of the Adare Basin [e.g., *Keller*, 2004] are shown within the section of Line 9. Description of the lithologies found within Site 273 follows *Hayes et al.* [1975b]. Ages above and below the unconformities for both DSDP sites are from *Savage and Ciesielski* [1983] and *Hayes et al.* [1975a].

4. Stratigraphic Framework

[14] The sedimentary sequence of the Ross Sea has been extensively imaged by numerous seismic reflection surveys. *Brancolini et al.* [1995] conducted the first comprehensive seismic stratigraphic study across the Ross Sea. They used single-channel and multichannel seismic reflection data compiled by the Antarctic Offshore Acoustic Stratigraphy (ANTOSTRAT) project to identify eight acoustic sequences (RSS1 to RSS8, from old to young) separated by key reflectors that were interpreted as major unconformities (RSU1 to RSU6, from youngest to oldest) (Figure 3a). This division was defined in the Northern Basin along a type section that crosses the shelf edge and enters the Adare Basin (Line IT 88 (Figure 2a); for cross sectional view please see Figure 4 of *Brancolini et al.* [1995]). The ANTOSTRAT sequence was correlated by *Brancolini et al.* [1995] to DSDP Leg 28 Ross Sea holes (270–273, continuously cored with 25% to 66% core recovery [*Hayes and Frakes*, 1975]) and drill sites MSSTS-1 and CIROS-1 (Figure 1). Ages of the sediments cored during DSDP Leg 28 were solely based on biological assemblages [*Hayes and Frakes*, 1975; *Savage and Ciesielski*, 1983].

[15] Further efforts in the last decade were focused on the seismic sequence within the VLB that was correlated with more recent drill sites (Cape Roberts Project (CRP) and ANDRILL sites [e.g., *Davey et al.*, 2000; *Fielding et al.*, 2008; *Johnston et al.*, 2008]). *Bart and Anderson* [2000] described in detail the late Neogene Northern Basin stratigraphy based on a single-channel seismic reflection survey. Recent studies have shown that the correlation of events across basement highs made between the various Ross Sea depocenters is problematic, especially for the old parts of the sequence (e.g., correlation of RSU6 between VLB and Northern Basin [*Davey et al.*, 2000]). Furthermore, the oldest seismic sequence that was directly sampled in the Northern Basin area (DSDP Site 273) is the early Miocene RSS4, making the age of the oldest parts of the sequence uncertain (Figure 3b).

[16] The stratigraphy of the Adare Basin has thus far been studied using a sparse set of MCS seismic lines. *Brancolini et al.* [1995] traced their stratigraphic facies from the Northern Basin down the continental slope and into the Adare Basin along a

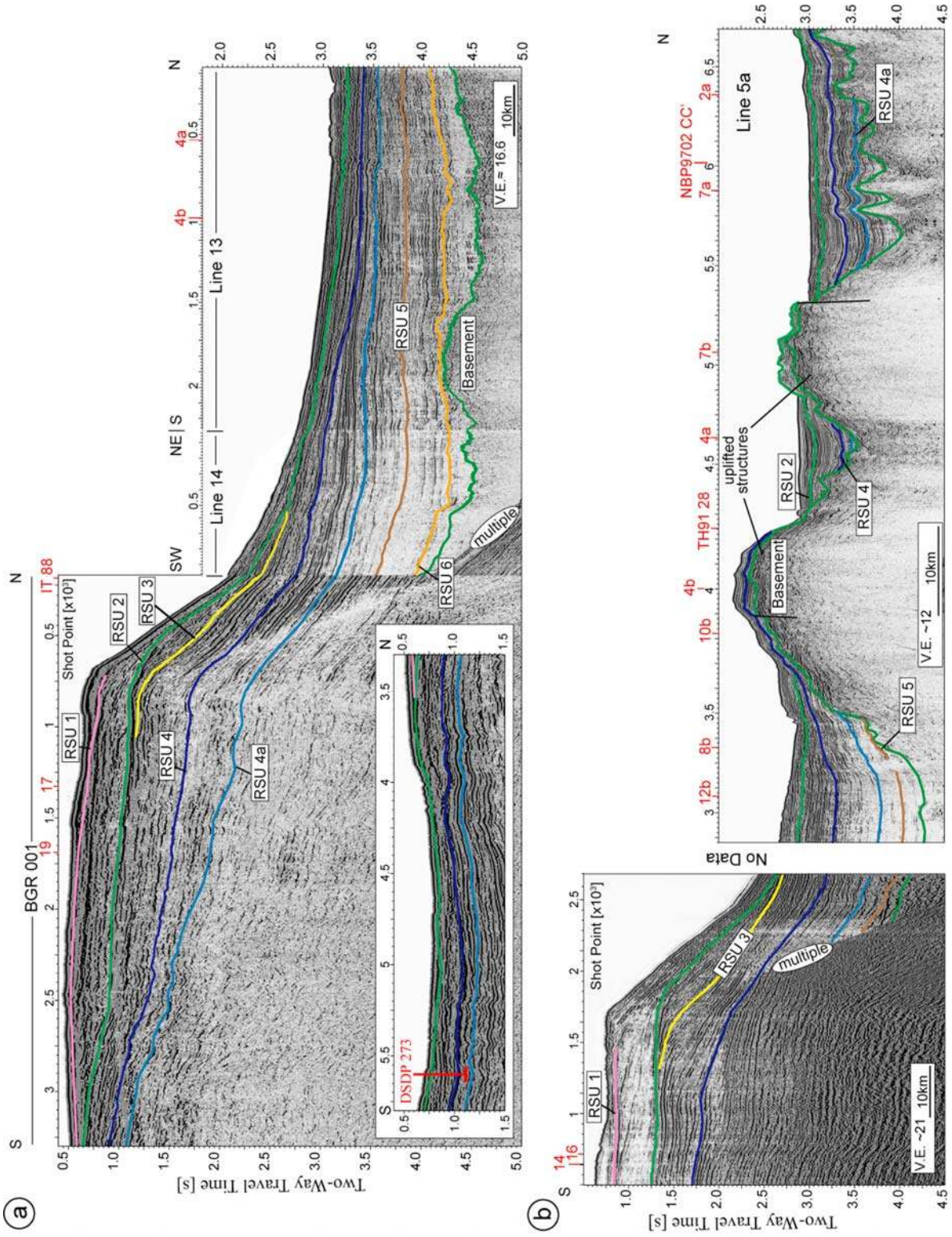
a
S
N
BGR 001
19
17
IT 88
Shot Point [x10³]
RSU 1
RSU 2
RSU 3
RSU 4
RSU 4a
RSU 5
RSU 6
Basement
multiple
SW
NE
Line 14
Line 13
4a
4b
V.E.≈ 16.6
10km
DSDP 273
Two-Way Travel Time [s]
b
S
14
16
Shot Point [x10³]
RSU 1
RSU 3
multiple
V.E. ~21
10km
No Data
N
NBP9702 CC
7a
6
2a
6.5
Line 5a
RSU 4a
RSU 2
RSU 4
RSU 5
Basement
uplifted structures
TH91 28
4b
4
10b
4.5
4a
5
7b
5.5
8b
3.5
12b
3
V.E. ~12
10km
Two-Way Travel Time [s]

Figure 4

ingle MCS line (Line IT 88, Figure 2a). Three east-west MCS lines collected during the NBP9702 cruise were used by *Keller* [2004] and subsequent studies [*Müller et al.*, 2005; *Whittaker and Müller*, 2006] to trace the sedimentary units across the Adare Trough. These studies used the sequence framework as defined at DSDP Site 274, located north of the Adare Basin [*Hayes et al.*, 1975a] (Figure 3b), and therefore their results were not directly aligned with the seismic framework of the Ross Sea. *Keller* [2004] and the later workers correlated horizons across prominent volcanic features and large-offset normal faults. These correlations have led, in places, to ambiguous results. Moreover, the temporal resolution of these interpretations is highly dependent on the depositional history at DSDP Site 274 where a thin sedimentary sequence contains a major unconformity between lithological units 3 and 4 of *Hayes et al.* [1975a] and seismic units SU2 and SU3 of *Keller* [2004] (Figure 3b). This unconformity has eliminated most of the Oligocene and early Miocene strata. We draw on these previous studies and use the newly acquired data set, together with the archival seismic digital data, to tie the seismic framework as defined by *Brancolini et al.* [1995] into and across the Adare Basin. A description of the seismic sequences used in our study is found in Appendix A and summarized in Figure 3a.

[17] Our correlation benefits from the relatively simple and continuous seismic characteristics that prevail from DSDP Site 273 toward the Adare Basin above RSU4a (e.g., Figure 4). The newly acquired seismic lines that cross the shallow Ross Sea shelf area allow us to confidently interpret horizons as primary arrivals down to 2.2–2.3 s two-way travel time (Figure 4). This depth typically encompasses the upper four unconformities (RSU1 to RSU4, middle Miocene and younger). We could not see basement in the shelf region, so it is not identified on any of the NBP0701 shelf lines. We correlated the deeper parts (deeper than RSU4) of the sequence into the Adare Basin following the correlation made by *Brancolini et al.* [1995] as defined along their type section (Line IT 88, note that our Line 14 follows the same exact track, Figure 2). As discussed in Appendix A, using basic seismic relationships (e.g., onlap and disappearance of seismic units on known age basement) we were able to confirm some of the assigned ages of *Brancolini et al.* [1995].

[18] To avoid unnecessary difficulties in our correlation, we do not correlate the ANTOSTRAT units across the entire Northern Basin but limit our interpretation to the area north of DSDP Site 273, where tie lines are available to link the stratigraphy into the Adare Basin (Figure 2a). A complementary tie line from DSDP Site 274 to the Adare Basin (Line 9, Figure 5) further constrains the correlation presented here. Our correlation contributes to the ongoing effort to create an updated regional seismic correlation across the Ross Sea and outer shelf area (ROSSMAP project, [*Davey and Sauli*, 2007]).

[19] The studied sedimentary sequence was deposited in diverse and evolving environments causing a pronounced variability in the seismic characteristics both spatially and temporally. These characteristics vary from the relatively simple, horizontally layered sequence within the shelf area (i.e., Northern Basin), to the outer slope where typically the seismic units display wedge-like prograding slope strata (Figure 4). Pronounced variability is found within the Adare Basin where an early Miocene tectonically controlled topography (Figures 6–9) modulated the depositional pattern and resulted in three major domains (discussed later in the text): west, east, and center. "Center" is defined as inside the Adare Trough and along the axis of deformation to the south-southwest of the trough. The lithologies found in DSDP Leg 28 drill holes and the seismic patterns shown in the MCS data suggest that the entire sequence was transported and

Figure 4. North-south seismic reflection profiles that run across the Northern Basin, shelf edge, and the Adare Basin. As for all of the seismic profiles shown in this manuscript, interpreted ANTOSTRAT seismic unconformities overlie the time migrated, exponentially gained seismic profiles. Intersections with other seismic profiles and drill sites are labeled with red. Vertical exaggerations (V.E.) are based on mean seismic velocity of 1800 m/s. (a) A mosaic tie line to DSDP Site 273 (BGR 001, Line 14, and Line 13 from south to north). Inset shows the southernmost part of BGR 001. The resolvable depth in the imaged shelf extends down to ~2.2 s, and therefore we interpret only unconformities above RSU4a. RSU5 and RSU6 were traced (and rechecked) across the shelf using IT 88 profile following *Brancolini et al.* [1995] and correlated into the Adare Basin from the crossing point. (b) Line 5a, a profile that runs along the center of the Adare Basin. Prograding clinoforms are notable above RSU3 across the outer shelf. The sedimentary sequence in the Adare Basin (SPs 3000–6500) onlaps onto the two uplifted structures indicating seafloor spreading–related formation.

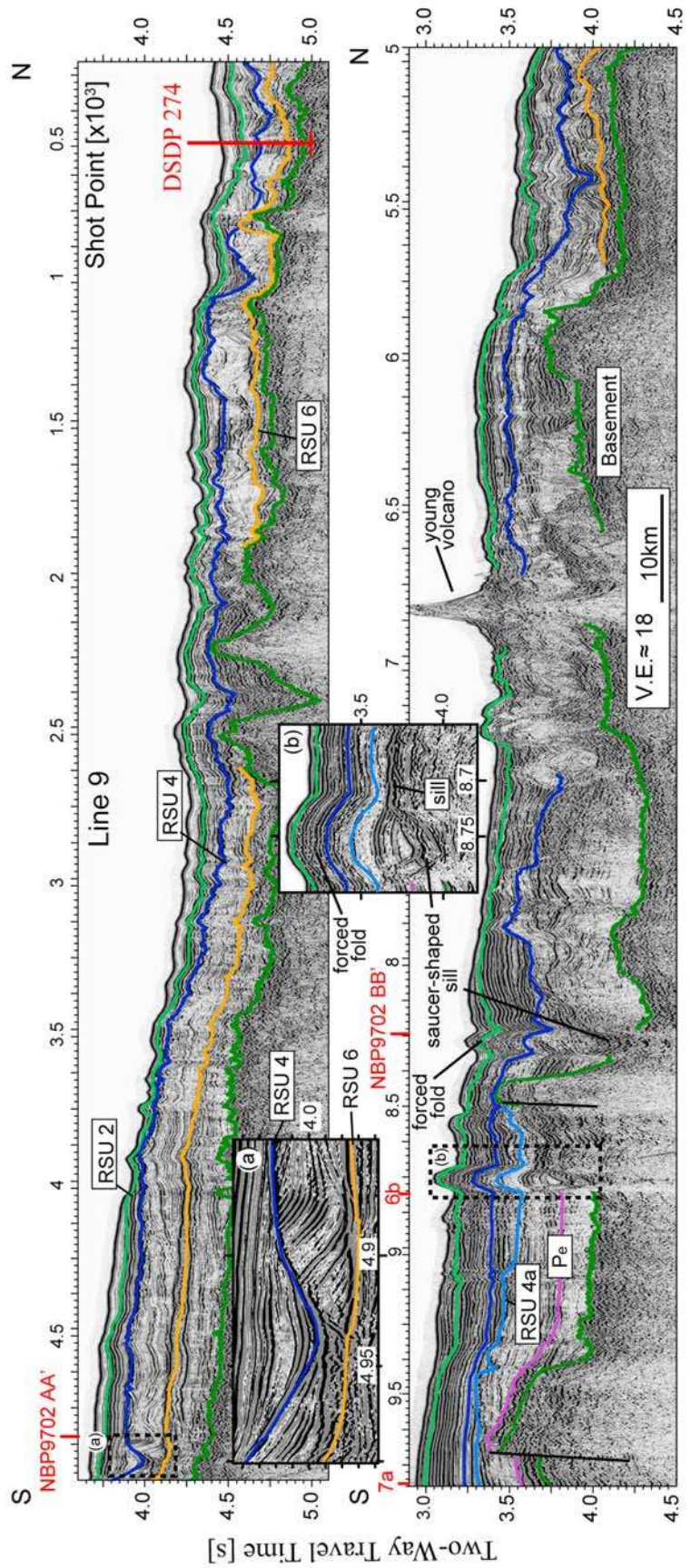

Figure 5. Tie line (Line 9) to DSDP Site 274, running east of the Adare Trough. RSU6 is truncated onto basement toward the Adare Trough (SP 5700). Igneous activity near SP 6800, together with complex sedimentary structures, prevents us from interpreting RSU4 at that location. Inset a is a close-up of RSU4 located above a block that underwent soft deformation (e.g., slumping). Inset b is a close-up of a saucer-shaped sill and its resultant forced fold. Note that the entire overlying sedimentary sequence is folded.

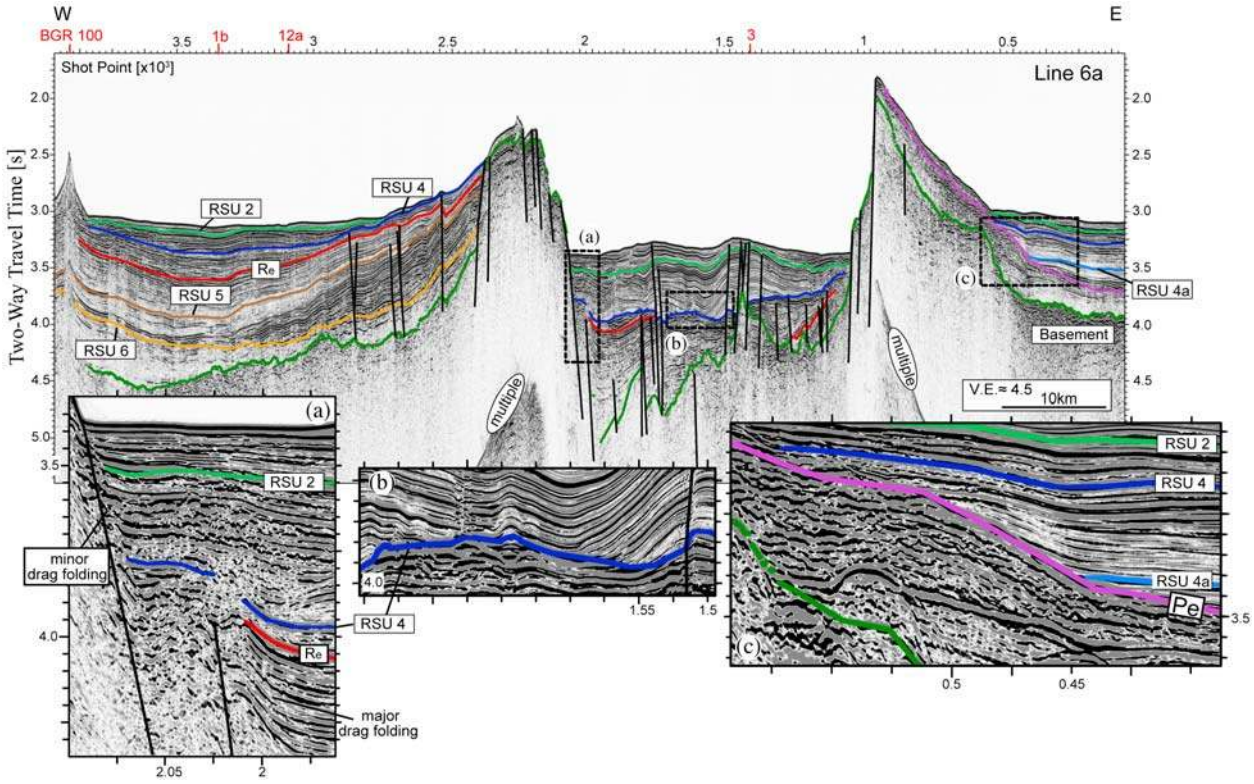

Figure 6. Line 6a, the northernmost profile across the Adare Trough, illustrating the asymmetric structure of the two flanks of the trough. Inset a is a close-up of the buried section of the main normal faults that border the western Adare Trough flank. Early Miocene faulting is most evident by drag-folded strata below the red unconformity. The overlying strata show relatively minor drag folding. Inset b is a close-up of the center of the Adare Trough. Below RSU4 are strong reflectors with chaotic to parallel reflector patterns suggesting reworked sedimentation. Above the unconformity are levee channel complexes suggesting gravity-controlled deposition. Inset c is a close-up of the base of the eastern flank. The purple unconformity marks the uplift of the flank with younger strata onlapping on top.

deposited within the Adare Basin through a combination of downslope gravity currents and deep water bottom currents resulting in turbidites and contourite drift deposits, respectively.

[20] Several pieces of evidence suggest that the majority of the filling sequence was transported into the basin, throughout the Neogene, from the south (i.e., Northern Basin): propagating and continuous reflectors found down slope from the Northern Basin (Figure 4), the onlapping of most of the strata onto the western shelf edge (i.e., east of Cape Adare, Figures 9–11), and the north-south alignment of isopachs within and near the basin (Figure 13). This property implies that the sequence in the Adare Basin is sensitive to the tectonic and climatic events that shaped the northwestern Ross Sea.

[21] The Adare Basin, prior to the postspreading tectonic deformational events, was probably characterized by a relatively low relief (up to 0.3 s two-way travel time, Figure 4). However, two major elevated crustal structures located at the youngest oceanic crust (Figure 2, SPs 4000 and 5000 in Figure 4b, and Figure 12b) confined the transported sediments to the western and eastern sides of the basin (Figure 13).

5. Discussion

[22] We will focus our discussion on the complex tectonic history of the Adare Basin in the temporal context of the following events: the early phase of postspreading deformation (Purple event, ~24 Ma), the major early Miocene rifting event (Red event, ~17 Ma), and the recent magmatic activity and vertical faulting (<5 Ma). We will then evaluate the results in the broad regional context.

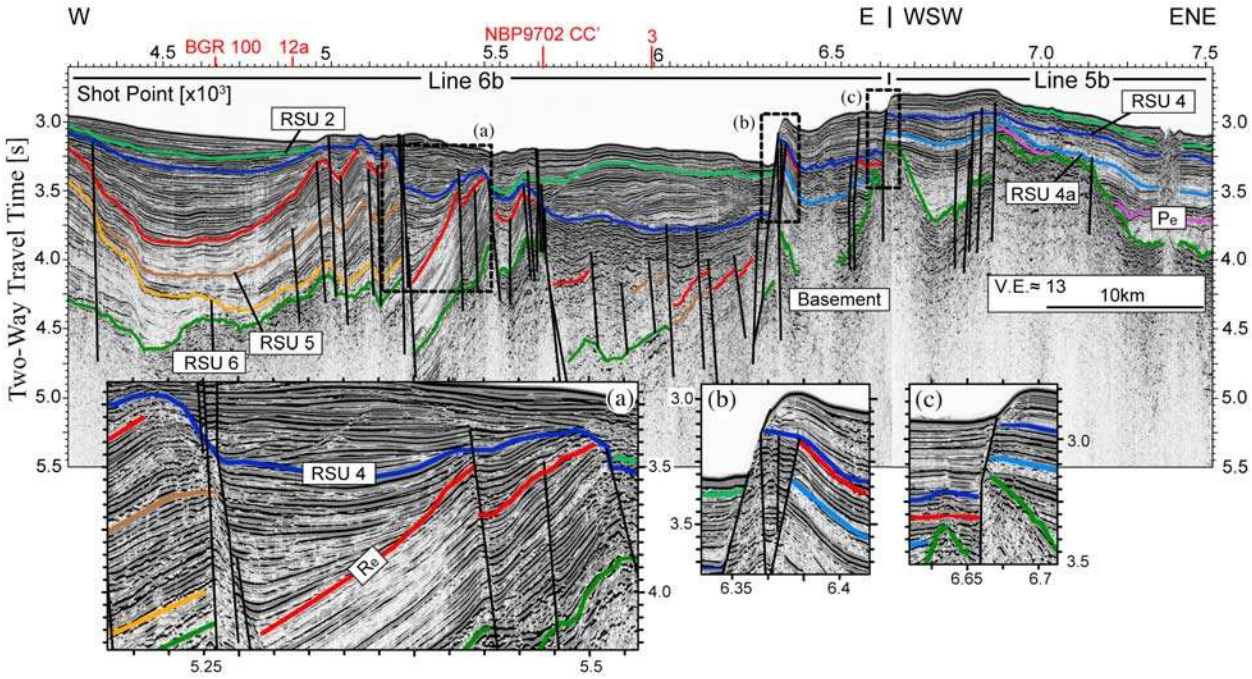

Figure 7. Mosaic of Lines 6b and 5b located immediately south of the Adare Trough. Inset a is a detail of a block-faulted area, located south of the terminated west flank of the Adare Trough. Note the onset of the early Miocene faulting event (Red event, Re) and the thick continuous synfaulting package that is overlain by RSU4. Extensional motion ceased subsequent to RSU4. Inset b is a close-up of a growth normal fault that bounds the early Miocene depression from the east. Red unconformity marks the onset of faulting, but developed seafloor scarp, younger drag folding, tilted strata, and thickening of strata away from the fault suggest that faulting was active continuously since the early Miocene. Note the large seafloor scarp (260 m). Inset c is a detail of a steep growth (and active) normal fault creating a seafloor scarp.

5.1. Late Oligocene Deformational Event: Purple Event

[23] The earliest evidence for onset of brittle deformation (Purple event) is shown by tilting of deep strata along a few prominent normal faults that strike NNW–SSE, parallel to the Adare spreading axis (e.g., Figure 9, inset b, and Figure 12), and are located within the center and eastern side of the Adare Basin (see dashed purple line in Figure 13c). The faults dip toward the paleo-spreading axis and therefore seem to reactivate preexisting structures. The typical vertical component of slip across the faults ranges between 0.2 and 0.5 s two-way travel time (Figure 9, SPs 6400, 7050, and 7350). The onset of faulting is found between RSU6 (~28 Ma) and RSU5 (~21 Ma, e.g., Figure 9, SPs 5300 and 6100–6400), and we therefore assign it to be of late Oligocene age [*Gradstein et al.*, 2004], at ~24 Ma. This speculative age coincides with a major unconformity found in the CRP drill core [*Wilson et al.*, 2000]. To this end, no direct observations exist to confirm whether this deformational event predates or postdates the cessation of seafloor spreading.

[24] The timing and nature of the formation of the Adare Trough had an important effect on the pattern of sediment supply in and near the Adare Basin. Tilted strata overlie the south part of the eastern flank of the Adare Trough (Figure 6, inset c). We could not identify similar deep tilted strata near the western flank of the trough. In fact, with the new reflection data set, we have correlated the seismic sequence across the Adare Trough by using the E–W profiles located south of the trough (Figures 2b, 7, and 8) and then using the N–S profiles (Figures A1 and A2). In this way we have traced the sequence back into and west of the trough. The resulting correlation indicates that the major faulting of the western Adare Trough flank is significantly younger than the purple unconformity found along the south part of the eastern flank. Our correlation suggests that the southeast corner high of the Adare Trough partly developed during the Purple deformational event (i.e., late Oligocene). We note however that the purple unconformity is

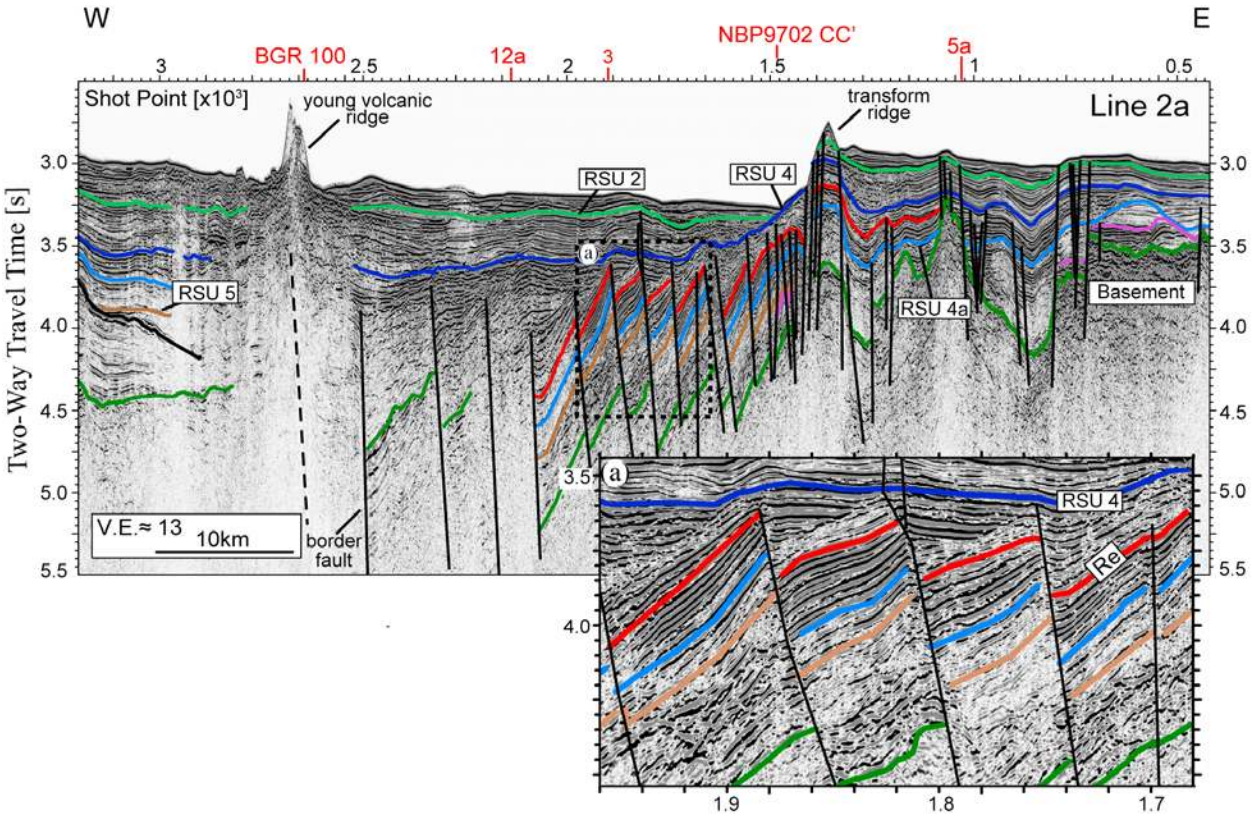

Figure 8. Line 2a crossing the morphological trough south of the Adare Trough. The morphological trough is bounded on the east by a transform ridge and by an active volcanic ridge on the west. Inset a is a close-up of tilted blocks bounded by east dipping normal faults. Faulting initiated at the Red event, prior to the middle Miocene RSU4 unconformity. Note the lack of extension above RSU4.

found south of the western flank (Figure 9, inset b). There, deep tilted strata are juxtaposed against east dipping normal fault. These deep tilted strata may indicate that fault reactivation during the Purple event may have been symmetric but cannot be detected along the western flank of the Adare Trough. The north part of the eastern flank is deeper than the southern edge (Figure 2). Although based on a limited amount of data collected across the northern part of the trough, onlapping of seismic reflectors onto the oceanic crust there [see *Müller et al.*, 2005, Figure 8] suggests that the northeastern flank represents the original shape of the trough, immediately after seafloor spreading ceased, and did not undergo significant uplift during the younger deformational events. Lack of sufficient MCS data led previous studies [*Müller et al.*, 2005; *Whittaker and Müller*, 2006] to conclude, solely based on gravity and flexural modeling, that the Adare Trough formed in a single event that took place shortly after spreading stopped. The new seismic data reveal that the formation of the trough was a rather complex process, both spatially and temporally.

[25] Contrasting seismic stratigraphies occur on the flanks of the Adare Trough. The western flank shows a complete and thick (~1.5 s two-way travel time) sequence whereas on the eastern flank a relatively thin (~0.7 s two-way travel time) and incomplete sequence is observed (Figure 6). These differences may result from the early uplift of the Adare Trough that channelized and forced the majority of sedimentation to take place west of the Adare Trough (Figure 13a).

[26] The asymmetric uplift of the trough may be related to the original asymmetry in seafloor spreading. This asymmetry may have produced contrasting mechanical crustal properties across the trough, causing a postspreading asymmetric response to induced stresses. The total motion along the reactivated faults (calculated by summing the horizontal separations across the faults) indicates that the Purple event resulted in a total of 1–2 km of extension over a distance of ~140 km, located across the center and eastern parts of the Adare Basin.

[27] A striking stratal relationship is found along the western continental slope (e.g., Figure 9, inset

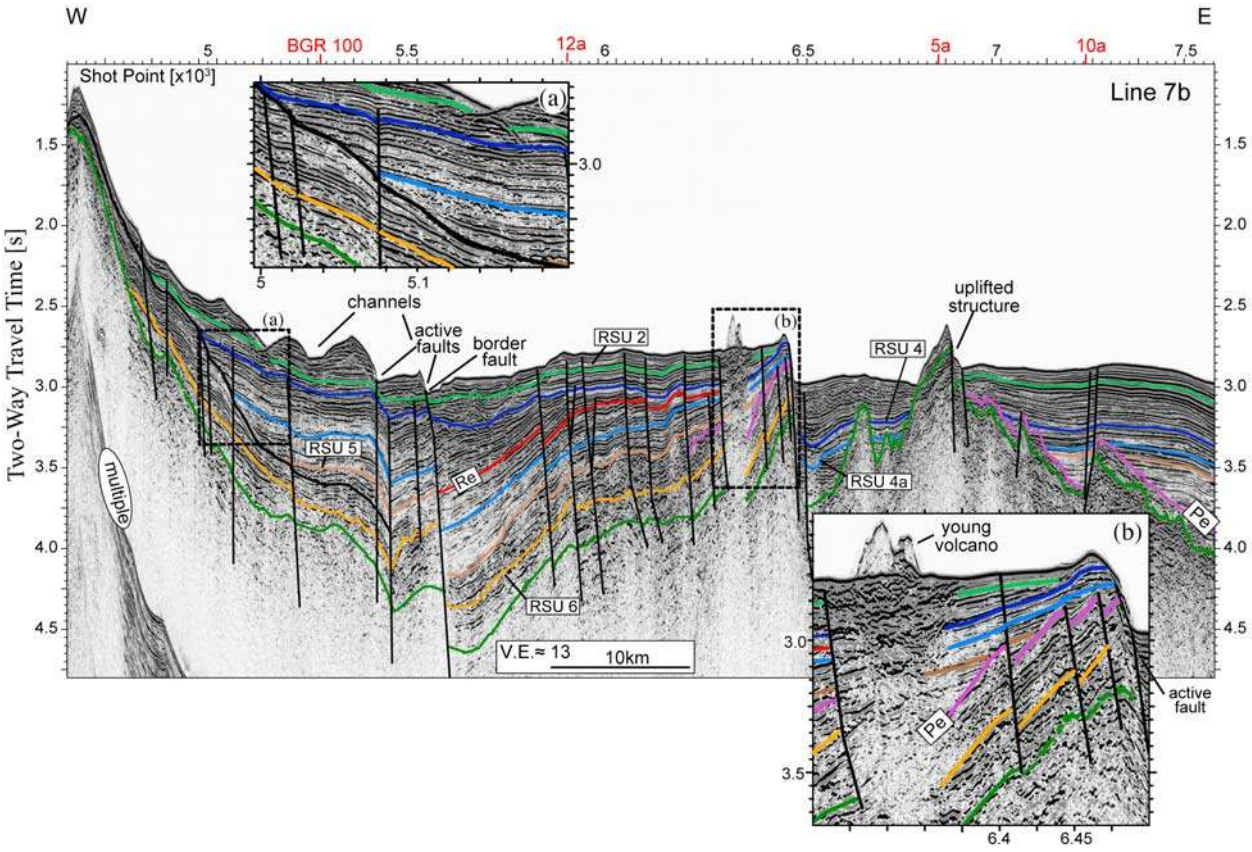

Figure 9. Line 7b crossing the center of the Adare Basin. This profile illustrates the three Neogene tectonic events of the Adare Basin. Evidence for early faulting (Purple event, Pe) is found across the entire profile (onset is marked by the purple unconformity). Additional major tilting event is found higher within the stratigraphic column (SPs 5500–5900, marked by red unconformity). Young volcanism and steep normal faulting mark the latest tectonic event (SPs 5900–6500). Inset a is a close-up showing an unconformity, marked by the thick black line, that separates eastward pinching out strata (below) from westward onlapping strata (above). This unconformity reflects a reorientation of deep water flow. Inset b is a close-up showing the tilting and faulting of the deep strata below the purple unconformity. The purple unconformity here marks an angular unconformity that resulted from tectonic tilting.

a, and Figure 10). There, an unconformity separates the deepest strata that pinches out eastward against an overriding younger strata that onlaps onto the unconformity. This event could have resulted from an important reorientation of bottom current flow, where an oblique SW to NE flow was replaced by a S to N flow. We could not directly confirm whether this unconformity correlates with the Purple unconformity, although we note that both unconformities are located in a similar position within the sedimentary package.

[28] The underlying mechanism that generated the Purple event, whether it is linked to motion within the WARS or formed independently, is of great interest. Similarity of seismic facies above and below the purple unconformity (e.g., Figure 9) suggests that the event was not associated with a pronounced change in the depositional environment. The throw along the faults diminishes southward without a resolvable throw found close to the southern continental slope (see Figure 11 versus Figures 9 and 10). On the other hand, the younger extensional motions after the Purple event, as we will discuss later in the text, show distinct linkage to faulting outside the basin and resulted in remarkably different extensional structures. We conclude that the Purple event was isolated from the extensional activity of the WARS.

[29] A number of independent observations provide important constraints on the tectonic process that resulted in the Purple event. The apparently abrupt cessation of seafloor spreading, without a slowdown in spreading rate toward the end [*Cande et al.*, 2000], might have left residual magma and heat in the Adare Basin. The temporal proximity of the Purple event to the end of seafloor

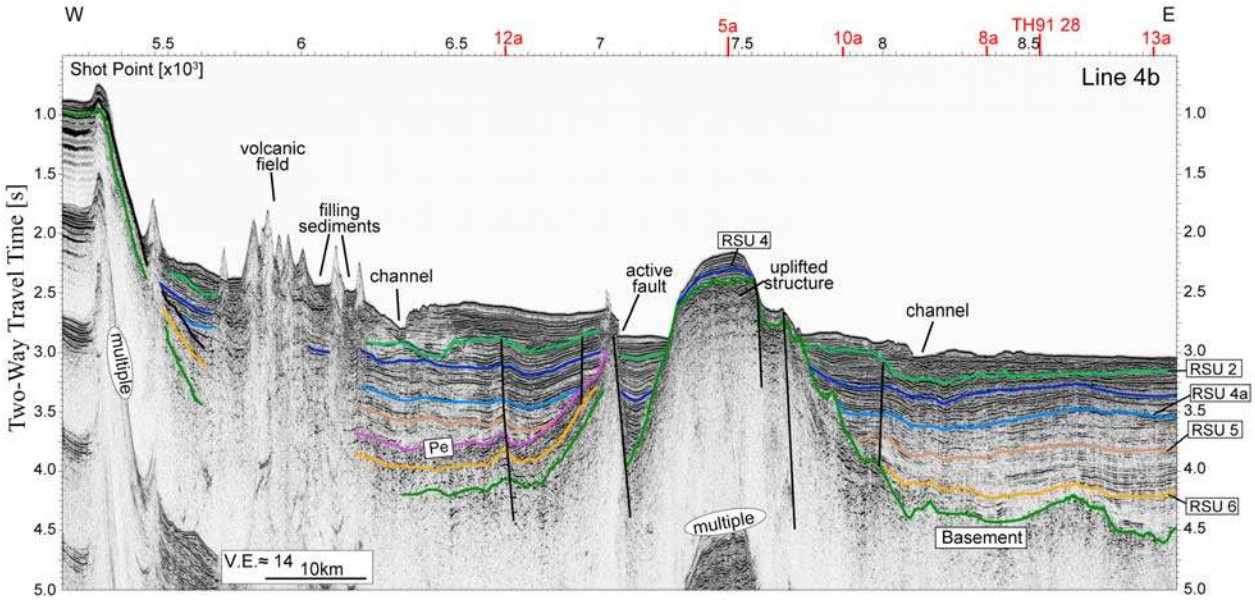

Figure 10. Line 4b crossing the southern Adare Basin. The purple unconformity can be traced across most of the basin while there are no indications for significant younger, Red event, faulting. Note the disappearance of RSU6 at the youngest part (i.e., center) of the basin. Young volcanism, channels, and an uplifted structure are pointed out.

spreading suggests that an excess of magma and heat could have led to reactivation of faults. In addition, local mantle convection has been suggested in the Gulf of Suez as a key component in shaping rift systems [*Steckler*, 1985] and an analogous process may also have been partly responsible for the creation of the Purple event.

5.2. Early Miocene Rifting: Red Event

[30] Evidence for the main phase of Neogene rifting (Red event) is found buried south and south-

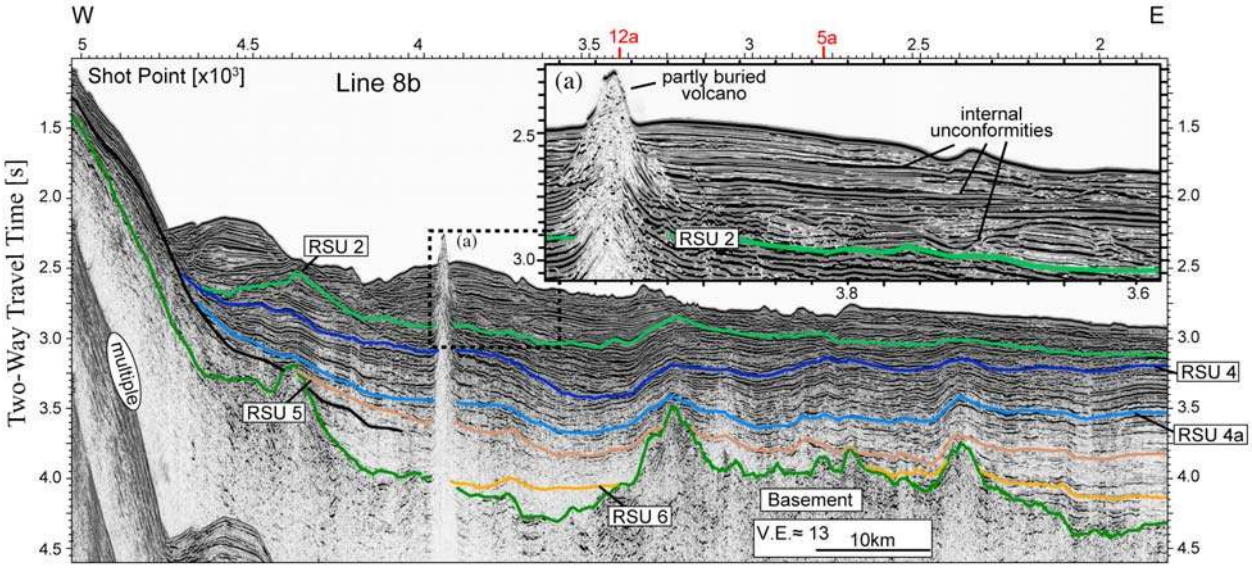

Figure 11. The southernmost crossing of the Adare Basin (Line 8b). Lack of faulting and continuous subhorizontal reflectors indicate that postspreading, Neogene faulting found within the central and northern parts of the Adare Basin did not continue into the southern part of the basin and, therefore, into the central part of the Northern Basin. Inset a is a close-up of the Pliocene strata overlying RSU2 showing internal unconformities. Note that the volcano is partly buried under the Pliocene strata.

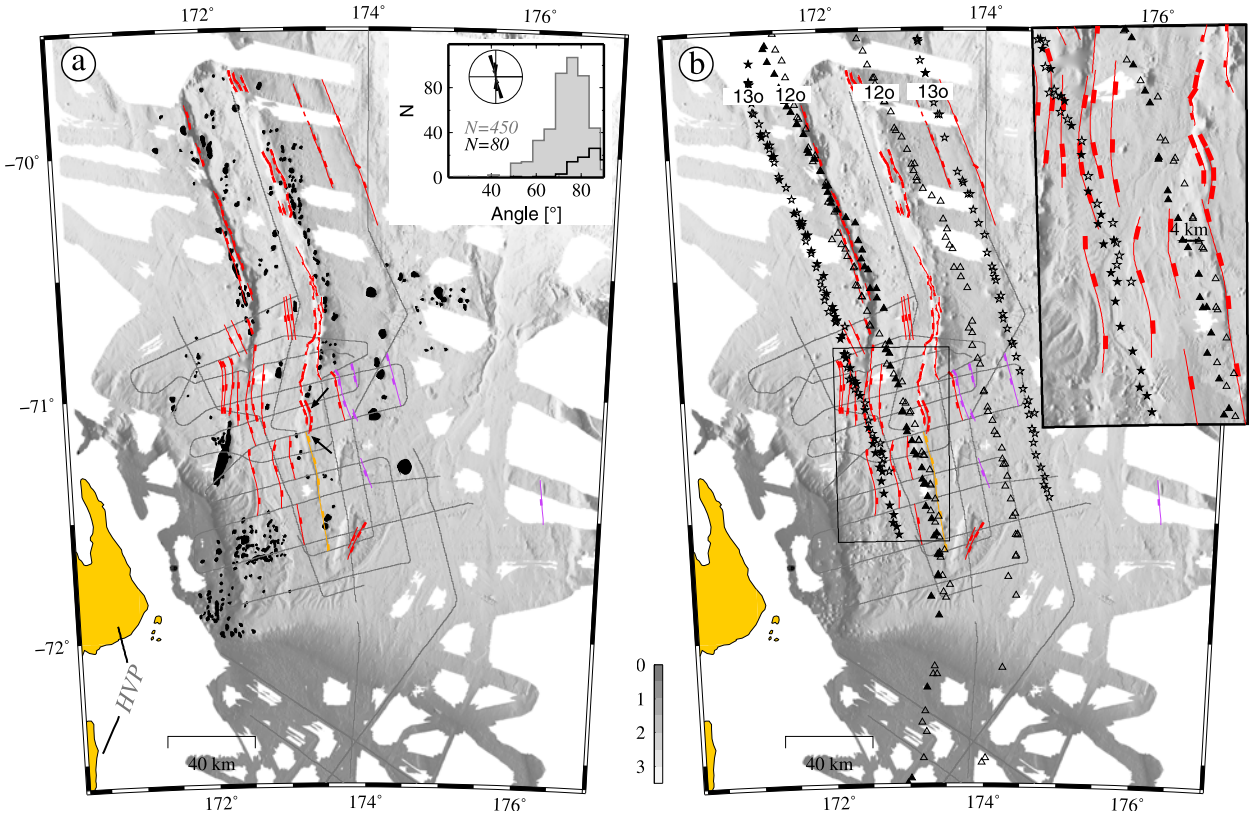

Figure 12. Summary map showing faults, volcanic features, and magnetic anomaly picks. Background topography (gray scale) is shown where multibeam data are available. (a) Structural map showing the faults that were interpreted on more than one seismic profile (red lines) and seafloor volcanic features (black) mapped using a combination of seismic and multibeam bathymetry data. Purple faults were active only in the late Oligocene deformational event whereas red faults were active during the younger, early Miocene, faulting event. The segments of faults that were active during both deformational events are shown with orange. Rectangular tabs mark the downthrown sides of the faults. The black arrows point toward the transfer ridge (northern arrow) and accommodation zone (southern arrow). Inset shows histograms with the apparent dip of all 450 interpreted faults (gray), and black histogram shows the true dip of the 80 faults that were interpreted on more than one seismic line. Strikes of these 80 faults are shown in the rose diagram with the maximum radius representing 30 fault segments. Typical strike of faults in the Adare Basin is N10°W. (b) Magnetic anomaly picks projected onto the structural map shown in Figure 12a. Picks for anomalies 13o and 12o are shown with stars and triangles, respectively. Empty (shaded) are the unrotated (rotated) picks. Rotations were made using the East-West Antarctica anomaly 18o rotation pole of *Davey et al.* [2006], with rotation angles of 1.26° and 2.4° for anomalies 12o and 13o, respectively. These angles are constrained by the northern sections of the isochrons, presumed to be outside the deformed zone. The misfit between the rotated and unrotated anomalies in the deformed zone suggests that the total extension, at the locations of the anomalies, could not have been larger than ~5 km.

west of the Adare Trough. This event, whose onset is marked by the red unconformity, documents the initiation of a series of similarly tilted fault blocks bounded by normal faults (Figures 6–9). The dips of the divergent reflectors above the red unconformity (Figure 7, inset a) display a continuous evolution, from dips subparallel to the red horizon (i.e., the bottom reflector) to the subhorizontal reflectors at the top of this package. These syn-faulting growth strata indicate that faulting was continuous during this tectonic interval. In general, normal faults are steep (>70°, using seismic velocity of 1800 m/s, Figure 12a). Typically, these faults dip eastward creating westward tilting half grabens (e.g., Figure 8, inset a). The tilt blocks form an en echelon pattern with an overall trend of NE–SW, from just south of the Adare Trough to the Cape Adare and Hallett volcanic province (Figures 12–14). The southwestern border of these structures reaches the slope of the western continental shelf.

[31] The onset of the Red event is stratigraphically located between unconformities RSU4a (~18.5 Ma)

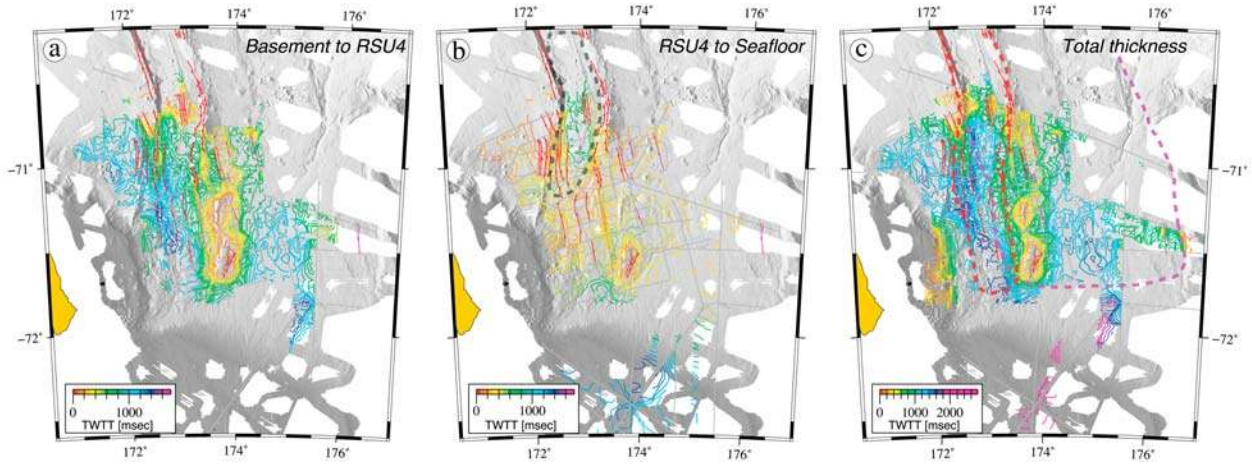

Figure 13. Isopach maps showing the cumulative thickness of the sedimentary packages from (a) basement to RSU4, (b) RSU4 to seafloor, and (c) total thickness. Also shown are the mapped faults. Contours (every 70 ms two-way travel time) were calculated based on an interpolated 1 km by 1 km grid of sediment thickness with a search radius of 16 km. Background topography (gray scale) is shown where multibeam data are available. Subsidence and fault-controlled sedimentation are apparent between the formation of the Adare Basin and RSU4. Younger sedimentation is controlled by the morphology of the basin (Figure 13b). The dashed gray line denotes the spatial extent of the gravity-controlled facies, deposited above RSU4 (Figure 13b). The spatial extent of the Purple and Red events are shown with dashed purple and red lines, respectively (Figure 13c).

and RSU4 (~16.5 Ma) (e.g., Figure 7, SPs 5200–5500, and Figure 8, SPs 1500–2000). We therefore speculate that deformation began at ~17 Ma (early Miocene). Growth strata are buried under RSU4 suggesting that all of the extensional activity ended prior to ~16 Ma. We note that the lack of drill sites within the Adare Basin, and the possibility of time transgressive unconformities, lead to some age uncertainties. Yet, since the ages above RSU4 at both DSDP 273 and 274 Sites are similar (Figure 3b), the Red event cannot be significantly younger than 17 Ma.

[32] Evidence for faulting and uplift is found along the western flank of the Adare Trough (e.g., Figure 6, SPs 2400–3000). Strata below the red unconformity are also tilted within the trough, adjacent to the westerly bounding faults (Figure 6, inset a), suggesting that the western flank uplifted during the early Miocene tectonic event. Uplift of the flanks of the Adare Trough is consistent with the change in lithology within DSDP Site 274, where particles coarser than silt size are absent above the middle Miocene sequence [*Hayes et al.*, 1975a], suggesting that the trough became an effective trap for terrigenous sediments, preventing them from reaching site 274 located on the northeast flank of the Adare Trough. The Red event involved the development of a new rift axis that ran from Cape Adare northeast to the Adare Trough and then turned north-northwest and reactivated the faults along the west flank of the Adare Trough. The topographically high southeast corner of the Adare Trough was at the bend in this new rift and was uplifted at the same time (supported by tilted strata found below the red unconformity, adjacent to the easterly bounding faults) (Figure 6, SPs 1100–1300). This early Miocene uplift marks the last prominent vertical motions that took place in the region of the trough. Younger motion along the bounding faults produced minor drag folding of the strata above the red unconformity (Figure 6, inset a). The vertical offset of RSU4 (~0.5 s two-way travel time) across the flanks suggests that up to ~450 m of additional uplift of the flanks occurred after the Red event.

[33] The tilted blocks south of the Adare Trough formed a narrow depression where sediments continued to be accommodated, but nevertheless resulted in the NE–SW trend of the present-day morphological trough (Figure 12). These tilted blocks are the cause of the disappearance of the Adare Trough to the south (Figure 14). They are bounded on the west by border faults (Figures 8 and 9) along which the throw is greatest. This structural asymmetry led to basins deepening westward, with thicker basin fill sequences toward the west (i.e., toward the border faults, Figure 13a). The

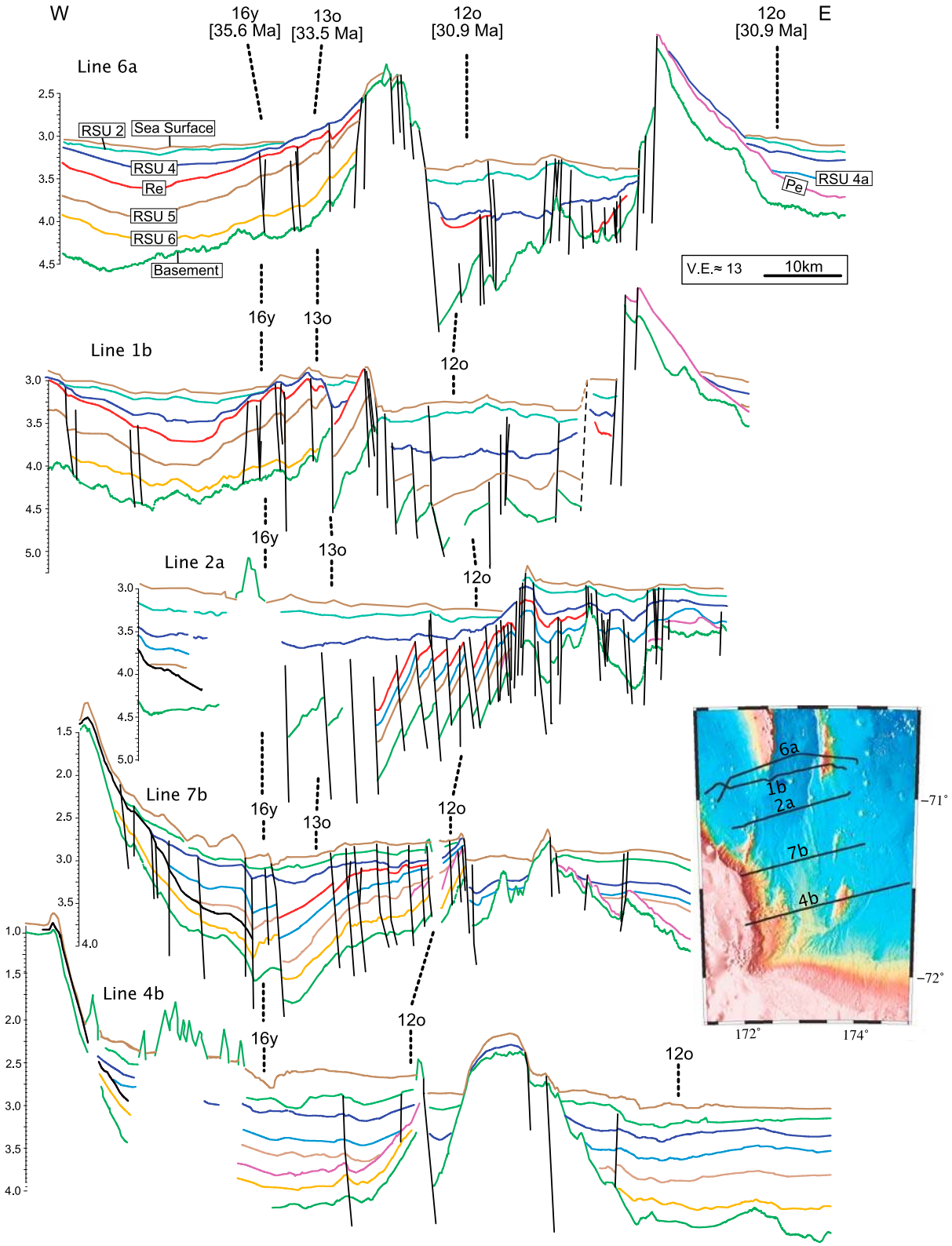

Figure 14. Schematic illustration of representative profiles ordered from north to south (top to bottom, respectively) and horizontally aligned according to their crossings with anomaly 16y of the East Antarctic plate (35.6 Ma [*Cande and Kent*, 1995]) that straddles the western part of the Adare Basin. Note the westward spatial propagation of the lower Miocene rifting event (i.e., Red event) from north to south. Also, note the disappearance of prominent faulting toward the south end of the Adare Basin. Inset map shows the location of these profiles.

spatial correlation between the faulting of the Red event and the filling sediment thickness (Figures 13a and 13b) suggests that rifting dominated the pattern of sedimentation.

[34] The spatial distribution of normal faults indicates a close association between the Adare rifting and the tectonics of the WARS, at least for its northern Victoria Land sector. The early Miocene rifting event marks a westward shift and localization (i.e., necking) of deformation within the Adare Basin, concentrating extension within a narrow (20 to 30 km wide, red dashed line in Figure 13c) deformed zone that cross cuts the basin. The landward trend of the rift suggests that deformation continued beyond the Adare Basin only to the southwest, probably on, or very close to, Cape Adare. Indeed, recent land-based structural mapping of *Faccenna et al.* [2008] showed that a set of NE–SW striking eastward dipping normal faults were active since the middle Miocene in the northernmost block of Victoria Land (Admiralty Mountains Block, Figure 1). This set of faults could have been linked with the deformation accommodated within the Adare Basin, transferring the motion southward, possibly into the Terror Rift. This structural setting hosted the younger volcanic activity (discussed further in section 5.3 [see also *Ferraccioli et al.*, 2009]). The lack of a southward continuation of faulting within the Adare Basin (Figure 11) implies that no deformation was accommodated within the center part of the Northern Basin during the Neogene, as supported by the study of *Brancolini et al.* [1995].

[35] Two dominant trends of normal faults are observed during the Red event. NNW–SSE (350°–170°, Figure 12) faults are located along the Adare Trough while N–S striking faults are found in the central part of the basin (Figure 12). The early Miocene direction of extension was therefore between ENE–WSW (80°–260°) and E–W presumably leading to, on some of these faults, minor strike-slip motion. The amount of extension that was accommodated during the Red event was calculated using the reflection data and verified independently by seafloor magnetic anomalies. An approximation of the extension along each of the seismic profiles that crosscut the extended zone was calculated using the sum of the heaves and, where tilted blocks are developed, using the apparent dips of the bounding faults and the tilted beds (using mean velocities of 1800 m/s [*Twiss and Moores*, 1992]). Our calculation along seven profiles that run E-W shows that the amount of extension in the early Miocene was between 3 and 5 km.

[36] The Eocene and Oligocene seafloor magnetic anomalies provide an independent constraint on the total amount of postspreading extension of the Adare Basin (i.e., the combined effect of the Purple and Red events). The West Antarctic plate isochrons (i.e., east side of the basin), located outside the deformed zone, serve as a reference for the pre-Neogene crustal setting. We have rotated back anomalies 12o and 13o using the anomaly 18o rotation pole of *Davey et al.* [2006], and the northern end of the East Antarctic anomalies, located outside the deformed zone, to constrain the degree of rotation (Figure 12b). Each anomaly was rotated using a single rotation angle (1.26° and 2.4° for anomalies 12o and 13o, respectively). The resulting mismatches between the rotated and unrotated anomalies, along the two trajectories straddling the deformed zone, confirms that the total amount of E–W extension, since the cessation of seafloor spreading, could not have been larger than ~5 km (see Figure 12b, inset). This result is in broad agreement with our seismic results and with the previous flexural uplift models for the Adare Trough of *Müller et al.* [2005]. We conclude that the total amount of extension in the Adare Basin was smaller than 7 km (Purple and Red events, combined), all of which occurred prior to the middle Miocene.

5.3. Recent Volcanism and Vertical Faulting: Pliocene to Present Day

[37] Prominent volcanic activity and near-vertical normal faults define the most recent tectonic activity in the Adare Basin. Based on the seismic reflection and bathymetric data, we have mapped 257 surface volcanic features (Figure 12a). Volcanism in the Adare Basin typically forms individual volcanic knolls (e.g., Figure 9, SP 6350). Some of the volcanic bodies have coalesced to build a volcanic ridge oriented NE–SW, following the general trend of the early Miocene deformed zone (Figure 12a). Part of the volcanism follows the trend of reactivated normal faults to form NNW–SSE chains, while other volcanic centers follow the major bounding faults of the Adare Trough (Figure 12a). Elsewhere, magma intruded at depth, forming subhorizontal sills and saucer-shaped sills that are always associated with forced folds and faults located immediately above the intrusions (e.g., Figure 5, inset b).

[38] Preliminary results from a recent geochemical study of dredged rocks from the Adare Basin [*Panter and Castillo*, 2007] reveal striking similarities between the lithological and isotopic signatures of the Adare volcanism and the on-land WARS volcanism. The spatial distribution of submarine volcanism within the Adare Basin (Figure 12a) seems to concentrate along the general direction of the Cape Adare volcanic ridge and the Hallett volcanic province. We therefore deduce that the volcanic activity within the Adare Basin is closely associated with the volcanic activity of the WARS, further confirming the linkage between the Neogene tectonic evolution of the Adare Basin and the WARS.

[39] The age of volcanism is constrained by both the seismic stratigraphic relationships and direct sampling of volcanic material. All of the volcanic knolls are exposed above the seafloor surface and penetrate nearly the entire stratigraphic column (i.e., no fully buried knolls are observed). In places, strata younger than RSU2 onlap onto these volcanic features (e.g., Figure 8, SP 2750, and Figure 11, inset a) suggesting a volcanic age older than 4 Ma. The entire stratigraphic section is folded above the imaged saucer-shaped igneous sills (e.g., Figure 5, inset b), without an onlapping pattern of younger reflectors on top, suggesting that they intruded the sedimentary sequence very recently [*Hansen and Cartwright*, 2006]. Preliminary ages (using $^{40}Ar/^{39}Ar$) of seven dredged volcanic sites, spread across a large distance, range from 0.2 to ~5 Ma [*Panter and Castillo*, 2008], further confirming a Pliocene age for the Adare volcanism. Although older volcanic activity in the Adare Basin is possible, we regard this option as unlikely as no such buried volcanic knolls, nor older intrusions, have been detected along the ~3,200 km of MCS data. Volcanism in the Hallett volcanic province ranges from 12.4 Ma south of Cape Adare [*Nardini et al.*, 2003], to 10–11 Ma for Cape Adare [*Mortimer et al.*, 2007]. The younger offshore ages indicate that the initiation of volcanism in the northern part of the WARS migrated northward, from the middle Miocene initiation at 73°S to the Pliocene initiation at 70°S.

[40] Pliocene to present-day brittle deformation is commonly found in areas that were active during the Red event. This activity is characterized by near-vertical normal faults that have, typically, minor throw (less than 0.1 s, e.g., Figure 6, inset b), although in a few places slip reaches 0.5 s and is accompanied with pronounced seafloor scarps (50 to 350 m, e.g., Figure 7, insets b and c). Growth faulting is also common (e.g., Figure 7, inset c), reactivating Neogene structures. The near-vertical orientation of these faults implies that this phase of deformation accommodated negligible extension compare with the earlier phases of deformation. A detailed analysis of the neotectonic activity in the Adare Basin will be presented elsewhere (J. M. Stock et al., manuscript in preparation, 2010).

5.4. Regional Synthesis

5.4.1. Implications for the Neogene Kinematics of the WARS

[41] The Neogene tectonic history of the Adare Basin as documented in this study has important implications for the kinematics of the WARS. We first make use of the Eocene-Oligocene kinematic framework (i.e., location of the pole of rotation) as a starting point to evaluate the Neogene motion of the WARS, assuming the rift system continued to extend in a coherent fashion. The cessation of spreading in the Adare Basin at ~26 Ma must have been associated with a sharp decrease in the WARS rate of extension, as no prominent extension is observed in the western Ross Sea basins and Adare Basin immediately after [*Cooper et al.*, 1987; this study]. Utilizing the Eocene-Oligocene East-West Antarctica pole of rotation (located near the South Pole [*Davey et al.*, 2006]), and our 3–5 km of early Miocene extension in the Adare Basin (the portion of the motion that appears to be linked with the regional framework), we predict that the extensional motion in the VLB sector should have been minimal (2–3 km) in the same period of time. A series of well constrained studies have shown that the VLB in the late Oligocene and early Miocene was indeed characterized by thermal subsidence without significant rifting [*Hall et al.*, 2007; *Henrys et al.*, 2007; *Fielding et al.*, 2008]. This kinematic confirmation implies that the position of the pole of rotation of the WARS was relatively stable from the Eocene until the middle Miocene.

[42] One of the most intriguing implications of this study is the difference in timing of extension in the Adare Basin compared to the region further south. The Adare Basin did not extend after the middle Miocene, a period when the Terror Rift accommodated 10 to 15 km of extension [*Henrys et al.*, 2007; *Fielding et al.*, 2008]. If the Eocene-Oligocene pole of rotation still prevailed, and the rift system still accommodated extension throughout its length in a coherent fashion, then 13 to 20 km of extension in the Adare Basin since the middle Miocene is ex-

pected. We regard this scenario as unreasonable and conclude that sometime in the middle Miocene (17–13 Ma) a major change in the kinematics of the WARS took place. At this moment, we cannot constrain the exact location of the middle Miocene and younger pole of rotation. Yet, near-zero extension in the Adare Basin, up to 5 km of extension in the northern Victoria Land (Admiralty Mountains Block), and 10 to 15 km of extension in the Terror Rift suggest an increase of rifting southward since the middle Miocene. The apparent northward propagation in the initiation age of volcanic activity in the late Neogene is consistent with this hypothesis (i.e., volcanism occurs first where the crust is more stretched).

[43] The suggested middle Miocene change in plate motion between East and West Antarctica has important implications on how we interpret some of the structural features found along the axis of the WARS. A recent study has suggested that deep subice troughs and basins located in the deep interior (e.g., Bentley Subglacial Trench, Figure 1) have formed under ice sheet conditions, implying Neogene formation [*LeMasurier*, 2008]. Based on the analysis of recently collected aerogravity data, *Jordan et al.* [2010] inferred low values of lithospheric rigidity under these buried basins, similar to the values inferred for active continental rift zones, confirming Neogene extension there. The kinematic evolution of these features is currently poorly understood, yet their recent formation suggests that rifting in the Neogene took place along most of the WARS length, probably with a southerly increasing magnitude. Therefore, the East-West Antarctica pole of rotation may have been located somewhere north of the Adare Basin since the middle Miocene (with opposite sense of motion compared to the Eocene-Oligocene motion). Alternatively, the nature of deformation in the WARS may have changed from coherent rifting (as in the Eocene-Oligocene period) to fragmented and kinematically isolated basins (for instance, the link between the Terror Rift and the northern Victoria Land is poorly resolved). The seemingly continuous Miocene faulting along the west margin of the WARS for hundreds of kilometers suggests, however, that the latter hypothesis is probably invalid. Geodetic [*Donnellan and Luyendyk*, 2004; *Zanutta et al.*, 2008] and seismicity measurements [*Evison*, 1967; *Behrendt et al.*, 1991] show that there is currently no significant motion across the WARS, suggesting that our hypothesized middle Miocene shift of the pole might have been the precursor to the unification of East and West Antarctica into a coherent plate.

[44] The uplift of the Transantarctic Mountains has been linked to the extensional motion accommodated within the rift system by isostatic uplift of the rift flank [e.g., *ten Brink et al.*, 1997] (but see other possible models therein). Neogene evolution of the Transantarctic Mountains is marked by contrasting denudation ages of its building blocks. Using cosmogenic isotopes, *Van der Wateren et al.* [1999] showed that the northern Victoria Land block was uplifted in the middle Miocene (minimum age of ~11 Ma, Figure 1) whereas the block located west of the Terror Rift, within central Victoria Land (Figure 1), was uplifted in the Pliocene (minimum age of ~4 Ma). Although these contrasting ages may have resulted from different glacial histories, variations in the characteristics of the crust, and/or dextral transtension that divided the continent into confined blocks [*Wilson*, 1995; *Salvini et al.*, 1997], they can also be partly explained by the two distinct rifting histories of the northernmost part of the WARS (i.e., Adare Basin) versus the WARS central part (i.e., Terror Rift). In this scenario, early Miocene rifting in the northwestern WARS was followed by the middle Miocene uplift phase of the Transantarctic Mountains northern block, and the middle Miocene opening of the Terror Rift was followed by the Pliocene uplift of the central Transantarctic Mountains.

[45] Cenozoic strike-slip reactivation of on-land NW–SE early Paleozoic structural features and offshore fracture zones in and near the WARS have long been suggested [e.g., *Salvini et al.*, 1997; *Storti et al.*, 2007]. A sparse set of seismic reflection data were used by *Storti et al.* [2007] to interpret flower structures in the Adare Basin as indicators for a major strike-slip fault that crosscut the basin along a NW–SE trend (termed the Cape Adare Fault by *Salvini et al.* [1997]). In addition, *Storti et al.* [2007] suggested that dextral motion have been transferred into the Adare Trough. Our imaged structural segments that created the en echelon fault pattern of the Red event are divided by small transfer zones (ridge and accommodation zones (Figure 12a), marked with black arrows). We find no seismic nor bathymetric evidence for a through going strike-slip fault, although minor strike-slip features might be located near the transfer zones. The marked continuity of seismic reflectors and seismic properties along our N–S profiles (Figures 4a and 4b) and E–W crossing basin profiles (e.g., Figures 6 and 11) provides

further support for the lack of strike-slip motion in the Adare Basin and on the continental slope. This observation agrees well with the continuity of the magnetic lineations that straddle the Adare Basin and Northern Basin without disruption (Figure 12b) [*Cande and Stock*, 2006; *Damaske et al.*, 2007]. Therefore, we argue that no major strike-slip faulting has occurred in the Adare Basin since seafloor spreading started (~43 Ma). A recent aeromagnetic survey over the northern edge of Antarctica (northern Victoria Land [*Ferraccioli et al.*, 2009]) demonstrated that Cenozoic alkaline intrusions located along the western margin of the Ross Sea are not significantly displaced by on-land NW–SE trending faults. Furthermore, significant strike-slip reactivation of the South East Indian fracture zones (as suggested by these studies) should have resulted in the misalignment of the reconstructed Australian plate magnetic anomalies onto their conjugate Antarctic plate anomalies, yet no such misfit is observed [*Cande and Stock*, 2004b]. Overall, these accumulating observations and inferences suggest that the magnitude of the hypothesized Cenozoic strike-slip motion was overestimated, both on land and offshore.

[46] A possible interplay between the tectonics of the WARS and climate has been suggested previously [e.g., *Behrendt and Cooper*, 1991; *Van der Wateren and Cloetingh*, 1999]. Crustal stretching may have promoted denudation of the Transantarctic Mountains which in turn provided part of the boundary conditions for ice sheet growth and consequent increase in erosion rates. Ice sheet growth then resulted in an increase in the supply of larger clasts of sediments into the rift system. It also may have created regional unconformities. Thus far, lack of drill cores within the Adare Basin precludes making any firm suggestion as to the time elapsed between the rifting phase (Red event) and the successive unconformity (RSU4), and also precludes investigating lithological changes across the unconformity and their likely relationship to climatic events.

5.4.2. Comparison With the Regional Tectonic Framework

[47] The suggested slow relative plate motion between the East and West Antarctic plates since the cessation of seafloor spreading, documented above, will have a negligible effect on the fit of the global plate circuit models (for instance, on the fit of the predicted track of the Hawaiian hot spot) and hence, for that purpose, the Antarctic plates can be treated as a single plate since chron C9. The proposed middle Miocene and younger motion within the WARS has, however, an important consequence on the predicted motion of the Alpine fault, New Zealand. Preliminary predictions of the motion along the fault, calculated using the Australia–East Antarctica–West Antarctica–Pacific plate circuit for Neogene time suggest that a decrease in the orthogonal motion across the fault would result from the extension within the WARS. The magnitude of decrease in orthogonal motion is currently unclear due to the large uncertainty in the location of the Miocene pole of rotation between East and West Antarctica. The increase of extension southward during the Miocene implies that, possibly, significant (>20 km) motion (either extension or strike-slip, depending on the location) was accommodated in the south parts of the rift system (e.g., within the subice troughs and offshore structures of the Bellingshausen Sea [*Müller et al.*, 2007]).

[48] The rifting history of the WARS should be associated with changes in plate motions of the adjacent plates. Cessation of spreading in the Adare Basin and the drop in the rate of rifting in the WARS at ~26 Ma was accompanied by a major plate reorganization south of New Zealand; the spreading direction on the Pacific-Australia ridge rotated significantly and was eventually replaced by oblique transform motion along the Macquarie ridge complex [*Sutherland*, 1995; *Massell et al.*, 2000; *Keller*, 2004].

[49] Neogene seafloor spreading along the Antarctic-Pacific ridge is marked by several well constrained major changes in plate motion [*Croon et al.*, 2008]. These events occurred at 27 Ma (chrons C9o-C9y), 23 Ma (chrons C6C-C6B), and 16 Ma (chrons C5Cy-C5b) and may have been related to the cessation of spreading along the Adare spreading ridge, the late Oligocene (Purple) deformational event, and the younger, early Miocene (Red) rifting event, respectively. A continuous change in plate motion since 16 Ma along the Pacific-Antarctic ridge suggests that the demise of rifting along the WARS was a gradual rather than an abrupt phenomenon. The close correlation of ages of changes in plate motion between the Antarctic-Pacific ridge and the Adare Basin provide an independent confirmation for our suggested Neogene temporal framework. The relative plate motions along the Antarctic-Australia ridge (South East Indian Ridge, SEIR, Figure 1), and between the Pacific and Australia plates (along

and near New Zealand) have been generally steady since 20 Ma [*Cande and Stock*, 2004b]. However, a significant change in plate motion has been detected around 6–8 Ma which triggered the formation of the Macquarie Plate and which is probably related to changes in the Pacific-Antarctic plate motions [*Cande et al.*, 1995]. At this point, the kinematics of the SEIR is known with insufficient temporal resolution (>5 Myr) to make a comparison with the WARS tectonics.

6. Conclusions

[50] Newly acquired seismic reflection and swath bathymetry data in the Adare Basin and the adjacent Ross Sea shelf reveal three major tectonic events. Based on correlation of the Ross Sea seismic stratigraphy of *Brancolini et al.* [1995] (ANTOSTRAT) from the Northern Basin into the Adare Basin we deduce the following:

[51] 1. A pulse of discrete normal faulting took place between the RSU6 and RSU5 unconformities, and is estimated at ~24 Ma. It is unclear whether this deformational event predates or postdates the cessation of seafloor spreading. Faulting resulted in negligible extension (less than 2 km) and did not seem to extend outside the basin. The southern part of the eastern flank and the western flank of the Adare Trough were uplifted during this event, probably reactivating a preexisting low-relief trough. This phase of deformation may have been linked with changes in the regional stress regime accompanying a reorganization of plate motion on the Pacific-Antarctic ridge.

[52] 2. A major localized early Miocene (between RSU4 and RSU4a, ~17 Ma) rifting event produced half grabens composed of west tilted blocks and east dipping normal faults that accommodated a total of 3–5 km of extension. Faulting resulted in the uplift of the western flank and southeastern corner of the Adare Trough, and subsidence south and southwest of the trough. The tilted blocks comprise an en echelon structural array with an overall NE–SW direction that starts south of the Adare Trough and approaches Cape Adare. Faulting reached the shelf edge, indicating that this event was probably linked with rifting activity outside the basin (most likely with the east dipping faulting in the northern Victoria Land [*Faccenna et al.*, 2008]).

[53] No motion is observed in the VLB during this interval [*Fielding et al.*, 2008], as expected given its proximity to the Eocene-Oligocene pole of rotation. Hence, we conclude that the pole of rotation between East and West Antarctica remained in the same location until (and including) the early Miocene (~17 Ma). This event marks the last prominent extension activity in the Adare Basin.

[54] 3. Penetrating the entire sedimentary sequence, igneous activity and steep normal faults mark the youngest phase (Pliocene to present day) of tectonic activity in the Adare Basin. Preliminary geochemical analyses of dredged basalts [*Panter and Castillo*, 2007], and the overall SW–NE spatial distribution of volcanic centers within and outside the Adare Basin indicate an intimate link to the Miocene volcanic activity found on land southwest of the basin. Steep normal faults produced prominent seafloor scarps but resulted in only a minor extensional component. At this stage, in terms of horizontal motion, the Adare Basin is nearly locked.

[55] The small amount of extension in the Adare Basin since the middle Miocene coeval with the opening of the Terror Rift [*Fielding et al.*, 2008], on-land Miocene normal faulting in the northern Victoria Land sector [*Faccenna et al.*, 2008], an extensional phase in the interior deep subice troughs and basins [*LeMasurier*, 2008], and a northward age propagation of the initiation of volcanic activity suggest that the pole of rotation between East and West Antarctica might have relocated north of the Adare Basin (with an opposing sense of motion relative to the Eocene-Oligocene poles). This requires an important middle Miocene (17–13 Ma) change in the relative plate motion between East and West Antarctica. Finally, good temporal correlation between these tectonic events and the kinematic framework of the adjacent Antarctic-Pacific ridge provides an independent confirmation of the time frame presented here.

[56] We find no indication for major strike-slip motion in and near the Adare Basin which confirms that no major dextral strike-slip faulting took place in the Adare Basin during the Neogene.

Appendix A: Seismic Sequences in the Northern and Adare Basins

[57] In Appendix A we present a summary of the seismic sequences as defined by *Brancolini et al.* [1995]. We expand their description to the Adare Basin as we make use of their seismic framework to constrain the timing of the tectonic events in the Adare Basin (Figure 3a). Using four across-shelf

(N–S) profiles and numerous across-basin (E–W) profiles (Figure 2) we are able to independently confirm their interpretation down to RSU4 at crossing points within both the Northern and the Adare basins. The age of RSU6 was verified independently using its onlapping position on oceanic crust of known age. The relationship between RSU2 and volcanism of known age constrains the maximum age of the unconformity. We are least confident of the age of RSU5, because no drill site is available and we were unable to find an independent age constraint.

A1. Seismic Sequence 1: Basement to RSU6

[58] Seismic Sequence RSS1 onlaps the acoustic basement and is separated from RSS2 by a prominent unconformity (RSU6) that can be traced continuously from the Northern Basin, down the continental slope, and within the southern and westernmost parts of the Adare Basin [*Brancolini et al.*, 1995, Figure 4] (Figure 6). Basement is characterized by strong low-frequency reflectors that strongly attenuate seismic energy (for example, see Figures 5 and 6, SPs 100–900). Identification of the basement-sediment contact was mostly straightforward. We did not attempt to interpret the contact in places of volcanic activity (e.g., Figure 7, SP 7400, and Figure 8, SP 2650), or in places with thick sedimentary sequences where the signal was severely attenuated (e.g., Figure 7, SPs 6050–6250). Subparallel reflectors characterize unit RSS1 and in places it is tilted by normal faults (e.g., Figure 7, SPs 4900–5100).

[59] RSU6 has never been directly sampled within the Northern Basin, and consequently its age was speculated by *Brancolini et al.* [1995] to be of middle Eocene to early Oligocene. However, drilling in the southwest of VLB demonstrated that the RSU6 age is ~17 Ma in the VLB area and, therefore, the miscorrelation of this unconformity between the basins is now widely accepted [*Davey et al.*, 2000]. RSU6 is found across most of the southern parts of the Adare Basin, except the youngest parts, where the unconformity onlaps the ~30 Ma oceanic crust (Figure 10) (ages are estimated using interpolation between magnetic anomaly picks, following the geomagnetic time scale of *Cande and Kent* [1995] (see Figure 14)). This suggests that the age of RSU6 as defined in the Northern Basin is near 30 Ma (early Oligocene) and therefore confirms the age assigned by *Brancolini et al.* [1995] and the miscorrelation of RSU6 between the Northern Basin and VLB.

[60] The upper boundary of the lowermost seismic unit (SU5 [*Hayes et al.*, 1975a]) of DSDP Site 274 (Figures 3b and 5, SPs 300–5700) corresponds to a prominent unconformity with chert below and silty clay-rich layers above [*Hayes et al.*, 1975a]. No biostratigraphic markers are available for this part of the drill hole to constrain its age. Yet, the drill site is located on crust of a known age (near anomaly 13o, ~33.5 Ma [*Cande and Kent*, 1995]) and the oldest, although uncertain, known sediment age (~31 Ma [*Hayes and Frakes*, 1975]) is located above this unconformity suggesting that the unconformity is of early Oligocene age. This age is broadly consistent with the age of RSU6 as defined at the Northern Basin and therefore we speculate that the unconformity that overlies SU5 at Site 274 corresponds with RSU6. This assignment has no effect on our overall correlation as this unconformity onlaps basement and disappears south of the drill site within the tie line (Line 9), before it is traced outward to other profiles (Figure 5, SP 5700).

[61] The lack of evidence for prominent subglacial erosion in the Northern Basin suggests that RSS1 was deposited under a temperate climate with rivers and wet-based mountain glaciers [*Brancolini et al.*, 1995].

A2. Seismic Sequence 2: RSU6 to RSU5

[62] Seismic Sequence RSS2 tends to show subhorizontal and continuous reflectors over the Northern and Adare basins (e.g., Figure 4a). In places where RSS1 is missing, this sequence onlaps the basement (Figure 4b). A major faulting event took place in the Adare Basin during the deposition of RSS2 (the onset of which is marked by the purple unconformity hereafter termed the Purple event (Pe) (Figures 3a and 6–11)). We define this horizon to mark the onset of faulting, below which the seismic reflectors are parallel, having uniform thickness. The purple unconformity, which is overlain by divergent and/or onlapping reflectors (Figure 6, inset c), is a time horizon that helps us correlate the top of RSS2 (RSU5) across faults and seismic discontinuities. We interpreted this horizon only in places where we observed this stratigraphic pattern and did not trace the event outward. The upper part of the sequence onlaps onto the Purple event without an appearance of any synfaulting

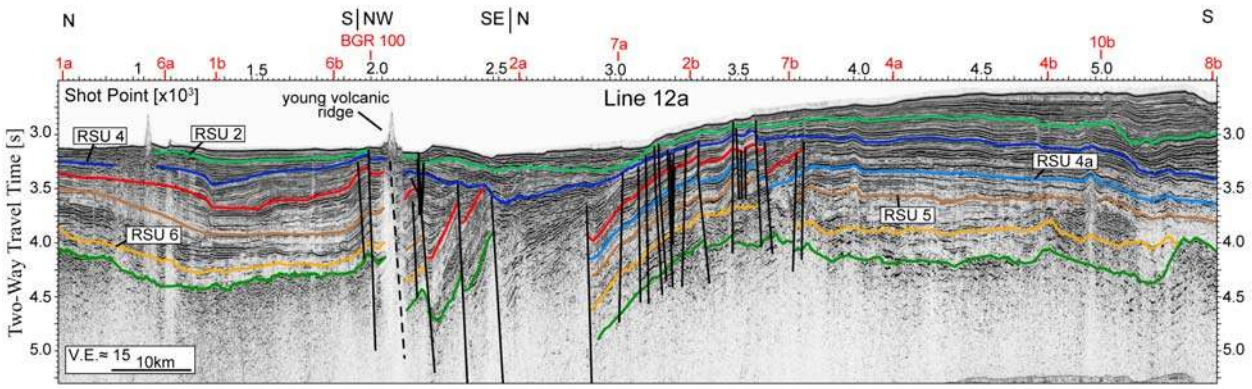

Figure A1. Line 12a, a N–S profile that runs along the western side of the basin. Note the localized zone of normal faulting and tilted blocks accompanied by depression (SPs 1900–3700). The red unconformity (lower Miocene) marks the initiation time of these structures.

divergent reflectors (e.g., Figure 9, SPs 5100 and 6100–6400), suggesting that this tectonic event produced major seafloor relief over a relatively short time interval. A major unconformity confined to the westernmost side of the Adare Basin is also found within RSS2 (black unconformity in Figure 9, inset a, and Figures 8–11). As discussed further later in the text, this unconformity resulted from reorientation of current activity.

[63] RSS2 has not been directly sampled in the Northern and Central basins area and was estimated to have occurred between 28 and 22 Ma [*Brancolini et al.*, 1995]. This time interval is missing from DSDP Site 274 and therefore, this unit is probably missing northeast of the Adare Trough, as confirmed in our tie line (Figure 5). *De Santis et al.* [1995] suggested that RSS2 was deposited in an open marine environment with humid and temperate climate conditions. Localized and near-shore grounding events [*Brancolini et al.*, 1995] suggest that glaciers were probably present in the Transantarctic Mountains and maybe in other land areas.

A3. Seismic Sequence 3: RSU5 to RSU4a

[64] In the Northern Basin and the Adare Basin, Seismic Sequence 3 (RSS3) downlaps, in places, on RSS2 and is generally conformable with the overlying and underlying units (Figures 4a, 10, and 11). Based on diatom assemblages for DSDP Site 273, *Savage and Ciesielski* [1983] have estimated the ages of RSS3 to range between 21 and 18.5 Ma. The low reflectivity and the uniform stratification of the sequence with buried channels offshore the VLB [*Brancolini et al.*, 1995] suggest that the sequence was deposited in an open marine environment with advance and retreat of subpolar glaciers into the continental shelf.

A4. Seismic Sequence 4: RSU4a to RSU4

[65] This seismic unit is found throughout most of the Northern and Adare basins. It contains subparallel, continuous, and well-defined reflectors (Figures 4a and 9–11). A major rifting event took place during the deposition of RSS4 (Figure 8, SPs 1100–2100, and Figure A1, SPs 2100–2400). This event is characterized by normal faulting that initiated, in places, differential block tilting and accompanying subsidence (Figures 7–9). This extensional event (onset of which is marked by red line termed the Red event (Re)) is typically associated with a pronounced upward change from a thick synrifting depositional sequence to a sequence of strong reflectors (Figure 7, SPs 5300–5400, and Figure 8, SPs 1500–2500). These strong reflectors exhibit, in places, chaotic structure that may suggest reworked sedimentation (e.g., Figure 8, SPs 1900–2300).

[66] The topmost part of the sequence (RSU4) is defined by a pronounced change from these strong reflectors to a less reflective or nonreflective sequence (e.g., Figure 6, inset a). In places, RSU4 is marked by an angular unconformity (e.g., Figure 6, inset a, and Figure 7, SP 5480). Along the eastern side of the Adare Basin, significant relief (up to 0.3 s two-way travel time) of RSU4 is associated with nonfaulted but internally deformed strata (e.g., Figure 5, inset a). These structures have probably formed by soft sediment deformation that initiated as a result of seismic activity associated with the red extensional event. Within and south of

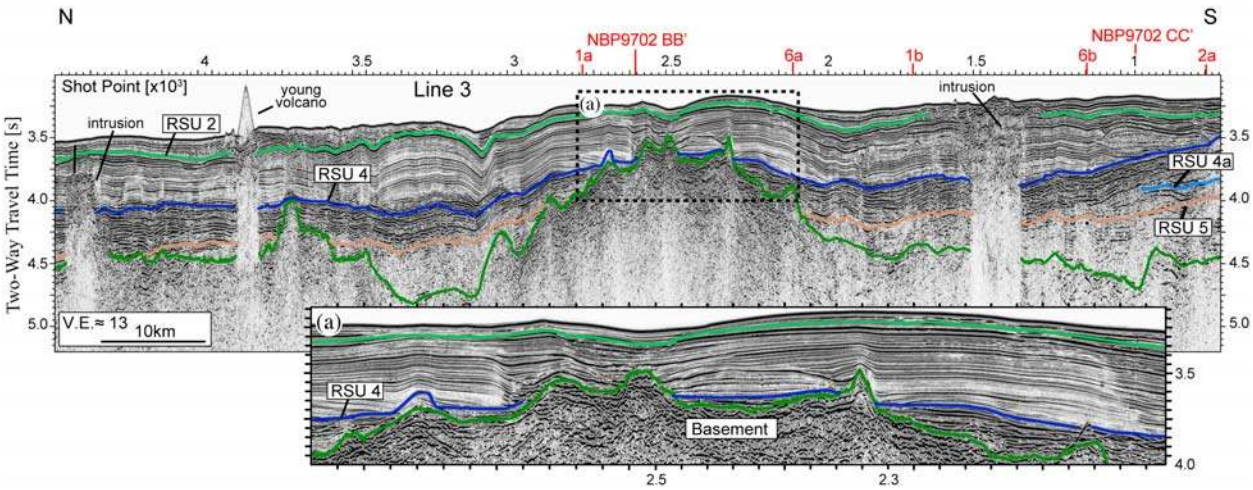

Figure A2. Line 3, a N–S profile located within the southern part of the Adare Trough. Inset a is a close-up showing the contrasting seismic properties of the seismic sequence across RSU4.

the Adare Trough, a change in the acoustic character across RSU4 together with its consistent appearance over tens of kilometers suggest that RSU4 is associated with a regional change in the sedimentation processes. This change might have resulted from a tectonically induced development of seafloor topography (e.g., developed depression) or to a climatic event. The nature of the Red event will be discussed further later in the text.

[67] RSS4 has been sampled at DSDP Sites 273, 272 and 274. In Site 273 it contains semilithified, diatom-bearing pebbly silty clay (Figure 3b). The top of the unit in Site 273 (RSU4) is made from a sand bed, which resulted, probably, from seafloor currents [*Brancolini et al.*, 1995]. The sequence was probably deposited under an open water environment that was followed by a change in ocean circulation and possibly the initiation of sea ice [*Savage and Ciesielski*, 1983]. *Brancolini et al.* [1995] assigned tentative ages to RSS4 between 18.34 and 16.5 Ma. Based on the biostratigraphic ages across the unconformity found at core 19, DSDP Site 274 (17 to 30 Ma [*Hayes et al.*, 1975a]), we assigned the RSU4 unconformity to the depth of 180.5 m at Site 274 (4.7 s two-way travel time in Figures 3b and 5).

A5. Seismic Sequence 5: RSU4 to RSU3/RSU2?

[68] RSS5 is mostly nonreflective, with irregular and crosscutting reflections in the Central and Northern basins [*Brancolini et al.*, 1995]. This sequence has been sampled at DSDP Site 273 where it contains semilithified, pebbly silty clay (Figure 3) [*Hayes et al.*, 1975b]. It was also sampled at DSDP Site 274 where it contains silty clay with scattered pebbles of highly varied lithologies that occur along the northern Victoria Land [*Hayes et al.*, 1975a]. Grains coarser than silt size are not observed above the middle of the sequence at Site 274, suggesting that the morphological Adare Trough may have developed sufficiently in the middle Miocene to be an effective trap for the gravity-controlled coarse sediments that were transported from the shelf and would have had to flow northeast across the Adare Trough to the location of Site 274. The youngest age below RSU3 at Site 273 is 14.7 Ma [*Savage and Ciesielski*, 1983].

[69] As discussed in the text, RSS6 is missing for most of the study area and RSU2 and RSU3 in the Adare Basin cannot be distinguished as separate seismic events. Within the Adare Trough, RSS5 displays a distinctive pattern of continuous parallel to subparallel or wedging low-amplitude reflections (Figure 6, SPs 1100–2000). These reflectors create channel-levee complexes (resembling the Amazon Fan–like complexes of *Manley and Flood* [1988]) indicating that sediment deposition was controlled by gravity currents. Downlap terminations that propagate northward along seismic Line 3 (Figure A2, SPs 2100 to 2700) suggest that the axes of these channels trend along the trough with a northerly direction of flow. The spatial extent of this gravity-controlled facies includes the morphological Adare Trough and the depressed region, located south-southwest of the trough (e.g., Figures 6, 7, and A2; see also dashed gray line in Figure

13b). The seismic properties of these deposits are highly variable over even a few kilometers. Generally, this unit is cut by near-vertical normal growth faults that typically display minor offsets and therefore resulted in a negligible extensional effect (e.g., Figure 6, inset b, and Figure 7, inset a). Accordingly, RSS5 marks the end of the pronounced extensional activity in the Adare Basin.

A6. Seismic Sequence 6: RSU3 to RSU2

[70] In the western Ross Sea RSS6 is observed only across the Northern Basin shelf break and is missing entirely from the rest of the Northern Basin (Figure 4a, SPs 1200 to 2600) [*Brancolini et al.*, 1995]. The steep slopes and rapid downlap of RSS6 near the base of the slope north of the Northern Basin suggest that the sequence was deposited during a sea level low stand. The age of this sequence is mostly speculative as it is missing from the shelf DSDP sites. *Brancolini et al.* [1995] have tentatively assigned RSS6 ages between 14 and 4 Ma. The last 10 million years of strata sampled at DSDP Site 274 (Figure 3b) [*Savage and Ciesielski*, 1983] show no biostratigraphic hiatus, suggesting that either the ages of RSS6 in the Adare Basin are 14 to 10 Ma or that the unit is not resolvable in the deep sea. We could not confidently identify RSS6 in the Adare Basin.

A7. Seismic Sequence 7: RSU2 to RSU1

[71] RSS7 is found across the entire study area and forms the uppermost observable strata. Typically, it exhibits uniformly stratified seismic reflectors (e.g., Figures 7 and 8), although in places multiple internal unconformities are observed (e.g., Figure 11, inset a). RSS7 was sampled by DSDP Sites 273 and 274. In Site 273 it includes glacial marine strata (sea ice conditions) dated between 4 and 2.8 Ma [*Savage and Ciesielski*, 1983]. Similar strata are found in Site 274, although no equivalent bounding unconformities were detected [*Hayes et al.*, 1975a]. In the western Ross Sea, the base of the sequence (RSU2) is marked by a sharp change in the erosional pattern, having wide and deep erosional troughs, similar to the morphology of the present-day seafloor. This observation provides the first clear evidence for full polar and ice sheet conditions [*Brancolini et al.*, 1995].

[72] In the Adare Basin, RSS7 is frequently penetrated by magmatic material (Figure 10, SPs 5800–6250). Several volcanic localities sampled during the NBP0701 cruise have been dated between 0.2 and 4.9 Ma [*Panter and Castillo*, 2008]. In places, RSU2 onlaps on similar volcanic features (e.g., Figure 8, SPs 2600–2750, and Figure 11, inset a).

A8. Seismic Sequence 8: RSU1 to Seafloor

[73] RSS8 is an isolated and typically thin sequence. In the Northern Basin a strong basal reflector that corresponds with RSU1 defines its base (Figure 4). At DSDP Site 273, the sequence consists of 0.8 m of marine sediments with ages ranging from 0.65 Ma to present day [*Savage and Ciesielski*, 1983]. No distinct appearance is found for RSS8 within the Adare Basin, suggesting that the unit thins below seismic resolution north of the shelf. DSDP Site 274 shows no indication of an RSU1 unconformity [*Hayes et al.*, 1975a], providing further evidence for the thinning and possible absence of RSS8 in the Adare Basin.

Acknowledgments

[74] We would like to thank Captain M. Watson, the crew, and the Raytheon staff of the R/VIB *Nathaniel B. Palmer* for their dedicated work during cruise NBP0701. Also, we thank Dietmar Müller and Sean Gulick for their helpful reviews; Neal Driscoll, Donna Blackman, and Jeff Gee for helpful discussions; Paul Henkart for the continuous help with SIOSEIS; and Chris Sorlein for introducing us to SPW software. Detlef Damaske is thanked for making the aeromagnetic data available for us. Interpretation of the seismic profiles was done with Kingdom Suite, a contribution of Seismic Micro-Technology. This project was funded by NSF grant OPP04-40959 (SIO) and OPP04-40923 (Caltech).

References

Anandakrishnan, S., and J. P. Winberry (2004), Antarctic subglacial sedimentary layer thickness from receiver function analysis, *Global Planet. Change*, *42*(1–4), 167–176.

Bart, P. J., and J. B. Anderson (2000), Relative temporal stability of the Antarctic ice sheets during the late Neogene based on the minimum frequency of outer shelf grounding events, *Earth Planet. Sci. Lett.*, *182*(3–4), 259–272.

Behrendt, J. C., and A. Cooper (1991), Evidence of rapid Cenozoic uplift of the shoulder escarpment of the Cenozoic West Antarctic rift system and a speculation on possible climate forcing, *Geology*, *19*(4), 315–319.

Behrendt, J. C., W. E. Lemasurier, A. K. Cooper, F. Tessensohn, A. Trehu, and D. Damaske (1991), Geophysical studies of the West Antarctic rift system, *Tectonics*, *10*(6), 1257–1273.

Behrendt, J. C., D. D. Blankenship, C. A. Finn, R. E. Bell, R. E. Sweeney, S. M. Hodge, and J. M. Brozena (1994), CASERTZ aeromagnetic data reveal late Ceonozoic flood basalts (?) in the West Antarctic rift system, *Geology*, *22*(6), 527–530.

Blackman, D. K., R. P. Von Herzen, and L. A. Lawver (1987), Heat flow and tectonics in the western Ross Sea, Antarctica,

in *The Antarctic Continental Margin: Geology and Geophysics of the Western Ross Sea*, edited by A. K. Cooper and F. J. Davey, pp. 179–189, Circum-Pac. Counc. for Energy and Nat. Resour., Houston, Tex.

Brancolini, G., A. K. Cooper, and F. Coren (1995), Seismic facies and glacial history in the western Ross Sea (Antarctica), in *Geology and Seismic Stratigraphy of the Antarctic Margin*, *Antarct. Res. Ser.*, vol. 68, edited by A. K. Cooper, P. F. Barker, and G. Brancolini, pp. 209–234, AGU, Washinghton, D. C.

Cande, S. C., and D. V. Kent (1995), Revised calibration of the geomagnetic polarity timescale for the late Cretaceous and Cenozoic, *J. Geophys. Res.*, *100*, 6093–6095.

Cande, S. C., and J. M. Stock (2004a), Cenozoic reconstructions of the Australia-New Zealand-South Pacific sector of Antarctica, in *The Cenozoic Southern Ocean: Tectonics, Sedimentation and Climate Change Between Australia and Antarctica*, *Geophys. Monogr. Ser.*, vol. 151, edited by N. F. Exon, J. K. Kennett, and M. J. Malone, pp. 5–18, AGU, Washington, D. C.

Cande, S. C., and J. M. Stock (2004b), Pacific-Antarctic-Australia motion and the formation of the Macquarie Plate, *Geophys. J. Int.*, *157*(1), 399–414.

Cande, S. C., and J. M. Stock (2006), Constraints on the timing of extension in the Northern Basin, Ross Sea, in *Antarctica: Contributions to Global Earth Sciences*, edited by D. Futterer et al., pp. 319–326, Springer, New York.

Cande, S. C., C. A. Raymond, J. Stock, and W. F. Haxby (1995), Geophysics of the Piman Fracture Zone and Pacific-Antarctic plate motions during the Cenozoic, *Science*, *270*(5238), 947–953.

Cande, S. C., J. M. Stock, R. D. Müller, and T. Ishihara (2000), Cenozoic motion between East and West Antarctica, *Nature*, *404*(6774), 145–150.

Cooper, A. K., and F. J. Davey (1985), Episodic rifting of Phanerozoic rocks in the Victoria Land Basin, western Ross Sea, Antarctica, *Science*, *229*(4718), 1085–1087.

Cooper, A. K., F. J. Davey, and J. C. Behrendt (1987), Seismic stratigraphy and structures in the Victoria Land Basin, Western Ross Sea, Antarctica, in *The Antarctic Continental Margin: Geology and Geophysics of the Western Ross Sea*, edited by A. K. Cooper and F. J. Davey, pp. 27–65, Circum-Pac. Counc. for Energy and Nat. Resour., Houston, Tex.

Croon, M. B., S. C. Cande, and J. M. Stock (2008), Revised Pacific-Antarctic plate motions and geophysics of the Menard Fracture Zone, *Geochem. Geophys. Geosyst.*, *9*, Q07001, doi:10.1029/2008GC002019.

Damaske, D., A. L. Läufer, F. Goldmann, H. D. Möller, and F. Lisker (2007), Magnetic anomalies north-east of Cape Adare, northern Victoria Land (Antarctica), and their relation to onshore structure, in *Antarctica: A Keystone in a Changing World—Online Proceedings of the 10th ISAES X*, edited by A. K. Cooper et al., *U.S. Geol. Surv. Open File Rep.*, *2007-1047*, doi:10.3133/of2007-1047.srp016.

Davey, F. J., and G. Brancolini (1995), The late Mesozoic and Cenozoic structural setting of the Ross Sea region, in *Geology and Seismic Stratigraphy of the Antarctic Margin*, *Antarct. Res. Ser.*, vol. 68, edited by A. K. Cooper, P. F. Barker, and G. Brancolini, pp. 167–182, AGU, Washinghton, D. C.

Davey, F. J., and L. De Santis (2006), A multi-phase rifting model for the Victoria Land Basin, western Ross Sea, in *Antarctica: Contributions to Global Earth Sciences*, edited by D. Futterer et al., pp. 303–308, Springer, New York.

Davey, F., and C. Sauli (2007), Antarctic sedimentary basins: Key to understanding glacial processes, *Eos Trans. AGU*, *88*(39), 384–385.

Davey, F. J., G. Brancolini, R. J. Hamilton, S. A. Henrys, C. C. Sorlien, and L. R. Bartek (2000), A revised correlation of the seismic stratigraphy at the Cape Roberts drill sites with the seismic stratigraphy of the Victoria Land Basin, *Terra Antarct.*, *7*(3), 215–220.

Davey, F. J., S. C. Cande, and J. M. Stock (2006), Extension in the western Ross Sea region-links between Adare Basin and Victoria Land Basin, *Geophys. Res. Lett.*, *33*, L20315, doi:10.1029/2006GL027383.

Della Vedova, B., G. Pellis, L. A. Lawver, and G. Brancolini (1992), Heatflow and tectonics of the western Ross Sea, in *Recent Progress in Antarctic Earth Science*, edited by Y. Yoshida, K. Kaminuma, and K. Shiraishi, pp. 627–637, Terra Sci., Tokyo.

De Santis, L., J. B. Anderson, G. Brancolini, and I. Zayatz (1995), Seismic record of late Oligocene through Miocene glaciation on the central and eastern continental shelf of the Ross Sea, in *Geology and Seismic Stratigraphy of the Antarctic Margin*, *Antarct. Res. Ser.*, vol. 68, edited by A. K. Cooper, P. F. Barker, and G. Brancolini, pp. 235–260, AGU, Washinghton, D. C.

Divenere, V. J., D. V. Kent, and I. W. D. Dalziel (1994), Mid-Cretaceous paleomagnetic results from Marie Byrd Land, West Antarctica: A test of post 100 Ma relative motion between East and West Antarctica, *J. Geophys. Res.*, *99* (B8), 15,115–15,139.

Donnellan, A., and B. P. Luyendyk (2004), GPS evidence for a coherent Antarctic plate and for postglacial rebound in Marie Byrd Land, *Global Planet. Change*, *42*(1–4), 305–311.

Elliot, D. H. (1992), Jurassic magmatism and tectonism associated with Gondwanaland break-up: An Antarctic perspective, in *Magmatism and the Causes of Continental Break-up*, edited by B. Storey, E. King, and R. Livermore, *Geol. Soc. London Spec. Publ.*, *68*, 165–184.

Evison, F. E. (1967), Note on the aseismicity of Antarctica, *N. Z. J. Geol. Geophys.*, *10*, 479–483.

Faccenna, C., F. Rossetti, T. W. Becker, S. Danesi, and A. Morelli (2008), Recent extension driven by mantle upwelling beneath the Admiralty Mountains (East Antarctica), *Tectonics*, *27*, TC4015, doi:10.1029/2007TC002197.

Ferraccioli, F., E. Armadillo, A. Zunino, E. Bozzo, S. Rocchi, and P. Armienti (2009), Magmatic and tectonic patterns over the Northern Victoria Land sector of the Transantarctic Mountains from new aeromagnetic imaging, *Tectonophysics*, *478*, 43–61, doi:10.1016/j.tecto.2008.11.028.

Fielding, C. R., S. A. Henrys, and T. J. Wilson (2006), Rift history of the western Victoria Land Basin: A new perspective based on integration of cores with seismic reflection data, in *Antarctica: Contributions to Global Earth Sciences*, edited by D. Futterer et al., pp. 309–318, Springer, New York.

Fielding, C. R., J. Whittaker, S. A. Henrys, T. J. Wilson, and T. R. Naish (2008), Seismic facies and stratigraphy of the Cenozoic succession in McMurdo Sound, Antarctica: Implications for tectonic, climatic and glacial history, *Paleogeogr. Paleoclimatol. Paleoecol.*, *260*(1–2), 8–29.

Fitzgerald, P. G., and E. Stump (1997), Cretaceous and Cenozoic episodic denudation of the Transantarctic Mountains, Antarctica: New constraints from apatite fission track thermochronology in the Scott Glacier region, *J. Geophys. Res.*, *102*(B4), 7747–7765.

Fitzgerald, P. G., M. Sandiford, P. J. Barrett, and A. J. W. Gleadow (1986), Asymmetric extension associated with uplift and subsidence in the Transantarctic Mountains and Ross Embayment, *Earth Planet. Sci. Lett.*, *81*, 67–78.

Gleadow, A. J. W., and P. G. Fitzgerald (1987), Uplift history and structure of the Transantarctic Mountains: New evidence from fission track dating of basement apatites in the Dry Valleys area, southern Victoria Land, *Earth Planet. Sci. Lett.*, *82*(1–2), 1–14.

Gradstein, F. M., et al. (2004), *A Geologic Time Scale 2004*, 589 pp., Cambridge Univ. Press, Cambridge, U. K.

Hall, J., T. Wilson, and S. Henrys (2007), Structure of the central Terror Rift, western Ross Sea, Antarctica, in *Antarctica: A Keystone in a Changing World—Online Proceedings of the 10th ISAES X*, edited by A. K. Cooper et al., *U.S. Geol. Surv. Open File Rep.*, *2007-1047*, doi:10.3133/of2007-1047.srp108.

Hampson, D. (1986), Inverse velocity stacking for multiple elimination, *J. Can. Soc. Explor. Geophys.*, *22*(1), 44–55.

Hansen, D. M., and J. Cartwright (2006), The three-dimensional geometry and growth of forced folds above saucer-shaped igneous sills, *J. Struct. Geol.*, *28*(8), 1520–1535.

Hayes, D. E., and L. A. Frakes (1975), General synthesis, Deep Sea drilling project Leg 28, *Initial Rep. Deep Sea Drill. Proj.*, *28*, 919–942, doi:10.2973/dsdp.proc.28.136.1975.

Hayes, D. E., et al. (1975a), Site 274, *Initial Rep. Deep Sea Drill. Proj.*, *28*, 369–433, doi:10.2973/dsdp.proc.28.110.1975.

Hayes, D. E., et al. (1975b), Site 273, *Initial Rep. Deep Sea Drill. Proj.*, *28*, 335–367, doi:10.2973/dsdp.proc.28.109.1975.

Heimann, A., T. Fleming, D. Elliot, and K. Foland (1994), A short interval of Jurassic continental flood-basalt volcanism in Antarctica as demonstrated by $^{40}Ar/^{39}Ar$ geochronology, *Earth Planet. Sci. Lett.*, *121*(1–2), 19–41.

Henrys, S., T. Wilson, J. M. Whittaker, C. Fielding, J. Hall, and T. Naish (2007), Tectonic history of mid-Miocene to present southern Victoria Land Basin, inferred from seismic stratigraphy in McMurdo Sound, Antarctica, in *Antarctica: A Keystone in a Changing World—Online Proceedings of the 10th ISAES X*, edited by A. K. Cooper et al., *U.S. Geol. Surv. Open File Rep.*, *2007-1047*, doi:10.3133/of2007-1047.srp049.

Huerta, A. D., and D. L. Harry (2007), The transition from diffuse to focused extension: Modeled evolution of the West Antarctic rift system, *Earth Planet. Sci. Lett.*, *255*(1–2), 133–147.

Johnston, L., G. S. Wilson, A. R. Gorman, S. A. Henrys, H. Horgan, R. Clark, and T. R. Naish (2008), Cenozoic basin evolution beneath the southern McMurdo Ice Shelf, Antarctica, *Global Planet. Change*, *62*(1–2), 61–76.

Jordan, T. A., F. Ferraccioli, D. G. Vaughan, J. W. Holt, H. Corr, D. D. Blankenship, and T. M. Diehl (2010), Aerogravity evidence for major crustal thinning under the Pine Island Glacier region (West Antarctica), *Geol. Soc. Am. Bull.*, *122*(5–6), 714–726.

Karner, G. D., M. Studinger, and R. E. Bell (2005), Gravity anomalies of sedimentary basins and their mechanical implications: Application to the Ross Sea basins, West Antarctica, *Earth Planet. Sci. Lett.*, *235*, 577–596.

Keller, W. R. (2004), Cenozoic plate tectonic reconstructions and plate boundary processes in the southwest Pacific, Ph.D. thesis, Calif. Inst. of Technol., Pasadena.

LeMasurier, W. E. (1990), Late Cenozoic volcanism on the Antarctic Plate: An overview, in *Volcanoes of the Antarctic Plate and Southern Oceans*, *Antarct. Res. Ser.*, vol. 48, edited by W. E. LeMasurier and J. W. Thomson, pp. 1–17, AGU, Washinghton, D. C.

LeMasurier, W. E. (2008), Neogene extension and basin deepening in the West Antarctic rift inferred from comparisons with the East African rift and other analogs, *Geology*, *36*(3), 247–250.

Luyendyk, B., S. Cisowski, C. Smith, S. Richard, and D. Kimbrough (1996), Paleomagnetic study of the northern Ford Ranges, western Marie Byrd Land, West Antarctica: Motion between West and East Antarctica, *Tectonics*, *15*(1), 122–141.

Lythe, M. B., and D. G. Vaughan (2001), BEDMAP: A new ice thickness and subglacial topographic model of Antarctica, *J. Geophys. Res.*, *106*(B6), 11,335–11,351.

Manley, P. L., and R. D. Flood (1988), Cyclic sediment deposition within the Amazon Deep-sea Fan, *AAPG Bull.*, *72*(8), 912–925.

Massell, C., M. Coffin, P. Mann, S. Mosher, C. Frohlich, C. Duncan, G. Karner, D. Ramsay, and J. Lebrun (2000), Neotectonics of the Macquarie Ridge Complex, Australia-Pacific plate boundary, *J. Geophys. Res.*, *105*(B6), 13,457–13,480.

Molnar, P., T. Atwater, J. Mammerickx, and S. Smith (1975), Magnetic anomalies, bathymetry and the tectonic evolution of the South Pacific since the late Cretaceous, *Geophys. J. Roy. Astron. Soc.*, *40*, 383–420.

Morelli, A., and S. Danesi (2004), Seismological imaging of the Antarctic continental lithosphere: A review, *Global Planet. Change*, *42*, 155–165.

Mortimer, N., W. J. Dunlap, M. J. Isaac, R. P. Sutherland, and K. Faure (2007), Basal Adare volcanics, Robertson Bay, North Victoria Land, Antarctica: Late Miocene intraplate basalts of subaqueous origin, in *Antarctica: A Keystone in a Changing World—Online Proceedings of the 10th ISAES X*, edited by A. K. Cooper et al., *U.S. Geol. Surv. Open File Rep.*, *2007-1047*.

Müller, R. D., S. C. Cande, J. M. Stock, and W. R. Keller (2005), Crustal structure and rift flank uplift of the Adare Trough, Antarctica, *Geochem. Geophys. Geosyst.*, *6*, Q11010, doi:10.1029/2005GC001027.

Müller, R. D., K. Gohl, S. C. Cande, A. Goncharov, and A. V. Golynsky (2007), Eocene to Miocene geometry of the West Antarctic rift system, *Aust. J. Earth Sci.*, *54*(8), 1033–1045, doi:10.1080/08120090701615691.

Nardini, I., P. Armienti, S. Rocchi, and R. Burgess (2003), $^{40}Ar–^{39}Ar$ chronolgy and petrology of the Miocene rift-related volcanism of the Daniell Peninsula (northern Victoria Land, Antarctica), *Terra Antarct.*, *10*(1), 39–62.

Panter, K. S., and P. Castillo (2007), Petrogenesis and source of lavas from seamounts in the Adare Basin, western Ross Sea: Implications for the origin of Cenozoic magmatism in Antarctica, in *Antarctica: A Keystone in a Changing World—Online Proceedings of the 10th ISAES X*, edited by A. K. Cooper et al., *U.S. Geol. Surv. Open File Rep.*, *2007-1047*.

Panter, K. S., and P. Castillo (2008), Petrology and source of lavas from seamounts in the Adare Basin, Western Ross Sea: Implications for the origin of Cenozoic magmatism in Antarctica, *Eos Trans. AGU*, *89*(53), Fall Meet. Suppl., Abstract V11F-05.

Rossetti, F., F. Storti, M. Busetti, F. Lisker, G. Di Vincenzo, A. L. Laufer, S. Rocchi, and F. Salvini (2006), Eocene initiation of Ross Sea dextral faulting and implications for East Antarctic neotectonics, *J. Geol. Soc. London*, *163*, 119–126.

Salvini, F., G. Brancolini, M. Busetti, F. Storti, F. Mazzarini, and F. Coren (1997), Cenozoic geodynamics of the Ross

Sea region, Antarctica: Crustal extension, intraplate strike-slip faulting, and tectonic inheritance, *J. Geophys. Res.*, *102*(B11), 24,669–24,696.

Savage, M. L., and P. F. Ciesielski (1983), A revised history of glacial sedimentation in the Ross region, in *Antarctic Earth Science*, edited by R. L. Oliver, P. R. James, and J. B. Jago, pp. 555–559, Cambridge Univ. Press, Cambridge, U. K.

Siddoway, C. S., S. L. Baldwin, P. G. Fitzgerald, C. M. Fanning, and B. P. Luyendyk (2004), Ross Sea mylonites and the timing of intracontinental extension within the West Antarctic rift system, *Geology*, *32*(1), 57–60.

Steckler, M. S. (1985), Uplift and extension at the Gulf of Suez: Indications of induced mantle convection, *Nature*, *317*(6033), 135–139.

Storti, F., F. Salvini, F. Rossetti, and J. P. Morgan (2007), Intraplate termination of transform faulting within the Antarctic continent, *Earth Planet. Sci. Lett.*, *260*(1–2), 115–126.

Sutherland, R. (1995), The Australia-Pacific boundary and Cenozoic plate motions in the SW Pacific: Some constraints from Geosat data, *Tectonics*, *14*(4), 819–831.

Sutherland, R., S. Spasojevic, and M. Gurnis (2010), Mantle upwelling after Gondwana subduction death explains anomalous topography and subsidence histories of eastern New Zealand and West Antarctica, *Geology*, *38*(2), 155–158.

ten Brink, U. S., R. I. Hackney, S. Bannister, T. A. Stern, and Y. Makovsky (1997), Uplift of the Transantarctic Mountains and the bedrock beneath the East Antarctic ice sheet, *J. Geophys. Res.*, *102*(B12), 27,603–27,621.

Truswell, E. M., and D. J. Drewry (1984), Distribution and provenance of recycled palynomorphs in surficial sediments of the Ross Sea, Antarctica, *Mar. Geol.*, *59*(1–4), 187–214.

Twiss, R. J., and E. M. Moores (1992), *Structural Geology*, Freeman, New York.

Van der Wateren, F. M., and S. A. P. L. Cloetingh (1999), Feedbacks of lithosphere dynamics and environmental change of the Cenozoic West Antarctic rift system, *Global Planet. Change*, *23*(1–4), 1–24.

Van der Wateren, F. M., T. J. Dunai, R. T. Van Balen, W. Klas, A. L. L. M. Verbers, S. Passchier, and U. Herpers (1999), Contrasting Neogene denudation histories of different structural regions in the Transantarctic Mountains rift flank constrained by cosmogenic isotope measurements, *Global Planet. Change*, *23*(1–4), 145–172.

Watson, T., A. Nyblade, D. A. Wiens, S. Anandakrishnan, M. Benoit, P. J. Shore, D. Voigt, and J. VanDecar (2006), P and S velocity structure of the upper mantle beneath the Transantarctic Mountains, East Antarctic craton, and Ross Sea from travel time tomography, *Geochem. Geophys. Geosyst.*, *7*, Q07005, doi:10.1029/2005GC001238.

Whittaker, J. M., and R. D. Müller (2006), Seismic stratigraphy of the Adare Trough area, Antarctica, *Mar. Geol.*, *230*(3–4), 179–197.

Wilson, G. S., et al. (2000), Chronostratigraphy of CRP 2/2A, Victoria Land Basin, Antarctica, *Terra Antarct.*, *7*, 647–654.

Wilson, T. J. (1995), Cenozoic transtension along the Transantarctic Mountains West Antarctic rift boundary, southern Victoria Land, Antarctica, *Tectonics*, *14*(2), 531–545.

Zanutta, A., L. Vittuari, and S. Gandolfi (2008), Geodetic GPS-based analysis of recent crustal motions in Victoria Land (Antarctica), *Global Planet. Change*, *62*(1–2), 115–131.